# IRG1 and iNOS act redundantly with other interferon gamma-induced factors to restrict intracellular replication of *Legionella pneumophila*.

Jordan V. Price[a#], Daniel Russo[a], Daisy X. Ji[b], Roberto Chavez[b], Lucian DiPeso[b], Angus Yiu-Fai Lee[c], Jörn Coers[d], and Russell E. Vance[b,c,e#]

Department of Biology, Oberlin College, Oberlin, Ohio, USA[a]; Division of Immunology & Pathogenesis, Department of Molecular & Cell Biology, University of California, Berkeley, California, USA[b]; Cancer Research Laboratory, University of California, Berkeley, California, USA[c]; Department of Molecular Genetics and Microbiology, Duke University Medical Center, Durham, North Carolina, USA[d]; Howard Hughes Medical Institute, University of California, Berkeley, California, USA[e].

Running head: Interferon gamma bacterial restriction

#Address correspondence to Jordan V. Price, jprice@oberlin.edu and Russell E. Vance, rvance@berkeley.edu

## Abstract

Interferon gamma (IFNγ) restricts the intracellular replication of many pathogens, but how IFNγ confers cell-intrinsic pathogen resistance remains unclear. For example, intracellular replication of the bacterial pathogen *Legionella pneumophila* in macrophages is potently curtailed by IFNγ, but consistent with prior results, no individual genetic deficiency we tested compromised IFNγ-mediated control. Intriguingly, however, we observed that the glycolysis inhibitor 2-deoxyglucose (2DG) partially rescued *L. pneumophila* replication in IFNγ-treated macrophages. 2DG inhibits glycolysis and triggers the unfolded protein response, but unexpectedly, it appears these effects are not responsible for perturbing the antimicrobial activity of IFNγ. Instead, we found that 2DG rescues bacterial replication predominantly by inhibiting the induction of two key antimicrobial factors, inducible nitric oxide synthase (iNOS) and immune responsive gene 1 (IRG1). Using immortalized and primary macrophages deficient in iNOS and IRG1, we confirm that loss of both iNOS and IRG1, but not individual deficiency in each gene, partially reduces IFNγ-mediated restriction of *L. pneumophila*. Further, using a combinatorial CRISPR/Cas9 mutagenesis approach, we find that mutation of iNOS and IRG1 in combination with four other genes (CASP11, IRGM1, IRGM3 and NOX2) results in a total loss of *L. pneumophila* restriction by IFNγ in primary bone marrow macrophages. There are few, if any, other examples in which the complete set of cell-intrinsic factors required for IFNγ-mediated restriction of an intracellular bacterial pathogen have been genetically identified. Our results highlight the combinatorial strategy used by hosts to block the exploitation of macrophages by pathogens.

## Importance

*Legionella pneumophila* is one example among many species of pathogenic bacteria that replicate within mammalian macrophages during infection. The immune signaling factor interferon gamma (IFNγ) blocks *L. pneumophila* replication in macrophages and is an essential component of the immune response to *L. pneumophila* and other intracellular pathogens. However, to date, no study has determined the exact molecular factors induced by IFNγ that are required for its activity. We generated macrophages lacking different combinations of IFNγ-induced genes in an attempt to find a genetic background in which there is a complete loss of IFNγ-mediated restriction of *L. pneumophila*. We successfully identified six genes that comprise the totality of the IFNγ-dependent restriction of *L. pneumophila* replication in macrophages. Our results clarify the molecular basis underlying the potent effects of IFNγ and highlight how redundancy downstream of IFNγ is key to prevent exploitation of the macrophage niche by pathogens.

## Introduction

Macrophages are preferred host cells for many species of intracellular bacterial pathogen. *Bona fide* pathogens of mammals, such as *Mycobacterium tuberculosis* (*Mtb*), *Listeria monocytogenes*, and *Salmonella enterica*, as well as environmental microorganisms that are "accidental" pathogens of mammals, such as *L. pneumophila*, display the ability to replicate efficiently in macrophages, demonstrating that these cells can provide a plastic niche suitable to the metabolic needs of distinct bacterial species (1). To defend against potential exploitation by diverse pathogens, including environmental microorganisms with which they have not co-evolved, macrophages require potent mechanisms to restrict intracellular bacterial replication. A cornerstone of the immune response to many intracellular pathogens is the cytokine interferon gamma (IFNγ). The importance of IFNγ is highlighted by the observation that genetic deficiencies in the IFNγ signaling pathway render humans highly susceptible to infections by intracellular pathogens, most notably *Mtb* and even normally benign environmental bacteria (2). Mice engineered to be deficient in the IFNγ pathway are also highly susceptible to intracellular bacterial pathogens, including *Mtb*, *L. monocytogenes*, *S. enterica*, *Brucella abortus*, and *L. pneumophila*, among others (3-9). Brown *et al* demonstrated that failure of IFNγ-deficient mice to control *L. pneumophila* likely occurs at the level of cell-intrinsic restriction of bacteria in monocyte-derived macrophages that infiltrate the lung following infection (10). Accordingly, *in vitro* infection models using bone marrow-derived macrophages (BMMs) have enabled meaningful study of the cell-intrinsic immune response to *L. pneumophila* coordinated by IFNγ. However, despite several decades of evidence supporting an essential role for

IFNγ in the antimicrobial immune response, the precise mechanisms by which IFNγ acts to mediate cell-intrinsic control of *L. pneumophila* and other pathogens remain obscure.

Inducible nitric oxide synthase (iNOS, encoded by the gene *Nos2* in mice) plays a key role in the IFNγ-dependent response to *Mtb* and several other pathogens (11-13). iNOS facilitates the production of nitric oxide (NO), a toxic metabolite with direct antimicrobial activity. NO also acts as a regulator of host responses and coordinates metabolic changes in IFNγ-stimulated macrophages (14-16). While *Nos2*$^{-/-}$ mice display increased susceptibility to infection by *Mtb*, it appears this is not simply due to direct cell-intrinsic antimicrobial effects of NO (17). In addition, the activity of iNOS is not absolutely required to control infection by many pathogens, suggesting that there are redundant iNOS-independent mechanisms that underlie the potency of IFNγ (18). Strikingly, while *L. pneumophila* does not display resistance to the effects of NO in broth, *Nos2*$^{-/-}$ macrophages are not impaired in IFNγ-dependent restriction of *L. pneumophila* (19-21). This indicates either that *L. pneumophila* is resistant to the effects of iNOS/NO during infection or, more likely, that there are redundant factors induced by IFNγ that can restrict *L. pneumophila* in the absence of iNOS.

Previous work has attempted to address the possibility of redundancy in the IFNγ-dependent immune response to *L. pneumophila*. Pilla *et al* generated quadruple knockout (QKO) mice deficient in *Nos2*, *Cybb* (cytochrome b(558) subunit beta, encoding NADPH oxidase 2 aka NOX2), *Irgm1* (immunity-related GTPase family M member 1), and *Irgm3* (immunity-related GTPase family M member 3), all induced by IFNγ (20). NOX2 partners with phagosomal oxidase components to generate reactive oxygen species, which, like NO, can cause direct toxicity to phagocytized pathogens in

neutrophils and macrophages (22, 23). IRGM1 and IRGM3 are antimicrobial GTPases that may participate in the disruption of membrane-bound, pathogen-containing compartments within phagocytes (20, 24). Remarkably, Pilla *et al* observed that macrophages derived from QKO mice retained potent restriction of *L. pneumophila* replication when stimulated with IFNγ, and further implicated the bacterial lipopolysaccharide detector caspase 11 (CASP11), which when activated can trigger host macrophage pyroptosis, in some of the residual IFNγ-dependent restriction of *L. pneumophila* replication in macrophages (20).

Recently, Naujoks *et al* implicated immune responsive gene 1 (IRG1, encoded by the gene *Acod1*) in the IFNγ-dependent immune response to *L. pneumophila*, demonstrating that driving *Acod1* expression in macrophages was sufficient to suppress *L. pneumophila* replication (21). However, the study did not address whether macrophages deficient in IRG1 were impaired in the ability to restrict *L. pneumophila* when stimulated with IFNγ. Like iNOS, IRG1 also generates a potentially toxic metabolite (itaconate), and contributes to metabolic changes that occur in inflamed macrophages (25-27).

*L. pneumophila* normally replicates in protozoan host amoebae, but can cause a severe pneumonia in humans, known as Legionnaires' disease, through infection of lung macrophages. *L. pneumophila* employs a type-IV secretion system to translocate bacterial effector proteins into the host cytosol, allowing the bacteria to establish an intracellular replicative compartment (28). Flagellin produced by wild-type *L. pneumophila* can trigger host cell pyroptosis via the NAIP/NLRC4 inflammasome; however, *L. pneumophila* that lack flagellin (Δ*flaA*) are able to replicate to high levels in

124 macrophages (29-35). We recently described a mutant strain of *L. pneumophila*
125 (Δ*flaA*Δ*uhpC*) that is able to replicate in macrophages treated with 2-deoxyglucose
126 (2DG), an inhibitor of mammalian glycolysis (36). This strain allows us to probe the role
127 that host cell metabolism plays in the immune response to *L. pneumophila*.
128 In the present study, we use a combination of pre-existing knockout mouse
129 models, pharmacological treatment with 2DG and other drugs, CRISPR/Cas9 genetic
130 manipulation of immortalized mouse macrophages, and BMMs from novel strains of
131 CRISPR/Cas9-engineered mice to survey of the factors required for IFNγ-dependent
132 restriction of *L. pneumophila* in macrophages. Ultimately, we demonstrate that iNOS
133 and IRG1 are sufficient and redundant in terms of IFNγ-dependent restriction of *L.*
134 *pneumophila*. Further, we identify six IFNγ-inducible factors: iNOS, IRG1, CASP11,
135 NOX2, IRGM1, and IRGM3, which are responsible for the entirety of the IFNγ-
136 dependent restriction of *L. pneumophila* in macrophages.
137
138 **Results**
139
140 **IFNγ restricts *L. pneumophila* replication across a spectrum of antimicrobial**
141 **gene-deficient macrophages.** In an attempt to identify specific factors that explain the
142 ability of IFNγ to restrict *L. pneumophila* replication in macrophages to specific genetic
143 factors associated with the immune response, we tested the ability of IFNγ to restrict *L.*
144 *pneumophila* in BMMs derived from various knockout mice. Using an extensively
145 validated strain of Δ*flaA L. pneumophila* that expresses luminescence (lux) genes from
146 *P. luminescens* (20, 36-38), we confirmed that Δ*flaA L. pneumophila* replicates in

147 unstimulated BMMs but does not replicate in BMMs stimulated with IFNγ (**Figure 1A**).
148 As expected, BMMs lacking the IFNγ receptor (*Ifngr*$^{-/-}$) do not restrict *L. pneumophila*
149 replication in the presence of IFNγ (**Figure 1B**). We confirmed that BMMs lacking
150 functional iNOS (*Nos2*$^{-/-}$) retain IFNγ-dependent restriction of *L. pneumophila* (**Figure**
151 **1B**) (19-21). BMMs lacking MYD88 (*Myd88*$^{-/-}$), a key adaptor in the innate inflammatory
152 immune response triggered by bacterial pattern recognition, and BMMs lacking MYD88,
153 NOD1, and NOD2 (*Myd88*$^{-/-}$ *Nod1*$^{-/-}$ *Nod2*$^{-/-}$), which do not activate inflammatory NF-
154 κB signaling in response to *L. pneumophila* (39), still restricted bacterial replication
155 when stimulated with IFNγ (**Figure 1C**). Consistent with previous results (20), BMMs
156 deficient in ATG5 (LysMCre$^{+}$ *Atg5*$^{fl/fl}$), a factor essential for autophagy (40), also
157 mediate IFNγ-dependent restriction of *L. pneumophila* replication (**Figure 1D**). Pilla *et al*
158 reported that guanylate binding proteins (GBPs) in conjunction with caspase-11
159 (CASP11) partially mediate IFNγ-mediated restriction of *L. pneumophila* in BMMs (20).
160 We observed that BMMs from mice that lack a region of chromosome 3 containing five
161 GBPs (GBP1, 2, 3, 5, and 7, *Gbp*$^{chr3\ -/-}$) and also BMMs that that lack functional
162 caspase-1 and CASP11 (*Casp1/11*$^{-/-}$) largely retain the ability to restrict *L. pneumophila*
163 in the presence of IFNγ (**Figure 1E**). Additionally, we observed that BMMs derived from
164 mice lacking functional MYD88 and TRIF (*Myd88*$^{-/-}$ *Trif*$^{-/-}$), STING (*Goldenticket*) (41),
165 IFNAR (*Ifnar*$^{-/-}$), and TNF receptor (*Tnfr*$^{-/-}$) all retained IFNγ-dependent restriction of *L.*
166 *pneumophila* replication (data not shown). In sum, these data confirm that no single
167 genetic factor studied to date is required to restrict *L. pneumophila* replication in
168 macrophages stimulated with IFNγ.

**2-deoxyglucose partially reverses IFNγ-dependent restriction of *L. pneumophila* in BMMs.** We next investigated the possibility that IFNγ may act to restrict *L. pneumophila* not through induction of any single antimicrobial factor but by changing the metabolic landscape of the host macrophage to be unsuitable for the metabolic needs of *L. pneumophila*. As macrophages infected with *L. pneumophila* and IFNγ-stimulated macrophages increase rates of glycolysis (1, 36, 42), we tested whether treatment with the glycolysis inhibitor 2-deoxyglucose (2DG) might interfere with IFNγ-dependent restriction observed in BMMs. 2DG is metabolized to 2DG-phosphate in cells, which is directly antimicrobial (36). However, by taking advantage of a newly identified strain of *L. pneumophila* resistant to the direct antimicrobial effect of 2DG(P) in BMMs (Δ*flaA*Δ*uhpC L. pneumophila*) (36), we observed that addition of 2DG to BMMs partially restored *L. pneumophila* replication in IFNγ-treated macrophages (**Figure 2A**). We confirmed that 2DG disrupts the enhanced glycolysis observed in *L. pneumophila*-infected BMMs stimulated with IFNγ (**Figure 2B**).

Previous studies have demonstrated that while *L. pneumophila* has the capacity to metabolize glucose, it does not rely on glucose or glucose derivatives to fuel its replication in broth, and is largely indifferent to perturbations in BMM glycolysis during infection (36, 43-45). To test whether induction of aerobic glycolysis by IFNγ restricts *L. pneumophila* replication, we performed infections using BMMs lacking hypoxia-inducible factor 1α (HIF1α), which fail to upregulate glycolysis in response to inflammatory stimuli and have a defect in IFNγ-mediated control of *Mtb* (14). We observed that HIF1α-deficient BMMs resembled wild-type BMMs in terms of IFNγ-dependent restriction and 2DG rescue of *L. pneumophila* replication (**Figure 2C**). Replacement of glucose with

galactose, which inhibits increased glycolysis in IFNγ-stimulated BMMs (14, 46), also did not alter the ability of IFNγ to restrict or 2DG to rescue *L. pneumophila* replication (**Figure 2D**). Further, IFNγ was able to mediate bacteria restriction, and 2DG was able to reverse this restriction, in BMMs cultured in glucose-free media lacking any added sugar (**Figure 2D**). Finally, we tested whether other inhibitors of glycolysis, 3-bromopyruvate (3BP) and sodium oxamate (NaO), recapitulated the effects of 2DG. Neither 3BP nor NaO reversed IFNγ-dependent restriction of Δ*flaA*Δ*uhpC L. pneumophila* (the 2DG-resistant strain) or Δ*flaA L. pneumophila* (**Supplementary Figure 1**). Together, these data indicate that glycolysis inhibition is not required for IFNγ-mediated restriction of *L. pneumophila* replication in BMMs, and suggests that effects of 2DG other than glycolysis inhibition are responsible for its interference with the cell-intrinsic IFNγ-dependent immune response to *L. pneumophila* in BMMs.

**Some, but not all, unfolded protein response stimuli reverse IFNγ-dependent inhibition of *L. pneumophila*.** To determine potential "off-target" effects of 2DG that could be responsible for reversal of IFNγ-mediated restriction of *L. pneumophila*, we performed transcript profiling on BMMs stimulated with the TLR2 agonist Pam3CSK4 or infected with *L. pneumophila*, stimulated with IFNγ ± 2DG. Pathway analysis of transcripts upregulated in 2DG conditions indicated induction of endoplasmic reticulum stress, also known as the unfolded protein response (UPR, **Supplementary Figure 2** and **Supplementary Table 1**). 2DG is thought to trigger the UPR due to interference with protein glycosylation pathways in the endoplasmic reticulum (47). This led us to hypothesize that induction of the UPR perturbs IFNγ-dependent restriction of *L.*

*pneumophila* replication in BMMs. In fact, we observed that other drugs that trigger UPR stress, including geldanamycin, brefeldin A, and dithiothreitol also partially rescued *L. pneumophila* replication in IFNγ-stimulated BMMs (**Figure 3A**). However, not all drugs that trigger the UPR rescued *L. pneumophila* replication in IFNγ-treated BMMs. For example, treatment of BMMs with the potent UPR inducers tunicamycin or thapsigargin did not affect IFNγ-mediated restriction of *L. pneumophila* replication (**Figure 3B**).

One effect of UPR stress is arrest of protein translation via the PERK/EIF2α pathway, which can be reversed by the drug ISRIB (48). Importantly, ISRIB treatment did not interfere with 2DG- or geldanamycin-mediated rescue of *L. pneumophila* replication in IFNγ-stimulated BMMs, indicating that reversal of IFNγ -mediated restriction does not result from a global block in translation (**Figure 3C**). We confirmed that UPR stimuli and ISRIB were inducing UPR-associated transcripts and inhibiting ATF4-associated transcripts, respectively, via global transcript profiling (**Supplementary Figure 3B**) (49). Taken together, these results suggest that while some UPR-triggering drugs can partially reverse IFNγ-dependent restriction of *L. pneumophila* replication in BMMs, induction of the UPR does not inherently interfere with IFNγ-mediated restriction. Additionally, the partial rescue of bacterial replication in IFNγ-stimulated BMMs by UPR-triggering drugs does not act exclusively through general inhibition of protein translation.

**IFNγ fully restricts *L. pneumophila* in BMMs lacking IRG1, but is only partially restrictive in BMMs lacking both IRG1 and iNOS**. Our analysis above revealed that certain UPR-stimulating drugs rescue *L. pneumophila* replication in IFNγ-stimulated

BMMs, while others do not. We speculated that we could use these stimuli as a filter to look for transcripts associated with a restrictive vs. permissive macrophage state. Using this logic to filter results from RNAseq analysis of BMMs stimulated with Pam3CSK4 ± IFNγ ± UPR stimuli, we identified two genes, *Nos2* (encoding iNOS) and *Acod1* (encoding IRG1), whose transcript levels were elevated in restrictive conditions and lowered in permissive conditions (**Supplementary Figure 4A** and data not shown). Since iNOS deficiency has no effect on IFNγ-mediated control of *L. pneumophila* replication (e.g. Figure 1B), we speculated that IRG1 may restrict *L. pneumophila* replication in IFNγ-stimulated BMMs, as suggested (but not directly tested) previously (21). Using immortalized BMMs derived from C57BL/6 mice that inducibly express Cas9 (iCas9), we targeted *Acod1* and *Ifngr* with guide RNAs to generate BMMs that lack expression of IRG1 and IFNγ receptor, respectively (**Supplementary Figure 5** and **Table 1**). In comparison with *Ifngr*-targeted BMMs, which fail to restrict *L. pneumophila* when stimulated with IFNγ, we observed that *Acod1*-targeted immortalized BMMs fully retained the ability to restrict *L. pneumophila* replication upon stimulation with IFNγ (**Figure 4A**). We next generated primary BMMs from *Acod1*$^{-/-}$ mice derived on the C57BL6/NJ background (26). Similar to immortalized BMMs, primary *Acod1*$^{-/-}$ BMMs displayed intact IFNγ-dependent restriction of *L. pneumophila* (**Figure 4B**). These results suggest that IRG1 activity alone is not required for restriction of *L. pneumophila* in IFNγ-stimulated macrophages.

We next tested the hypothesis that iNOS and IRG1 activity are redundant in terms of effecting restriction of *L. pneumophila* in IFNγ-stimulated BMMs. In line with this hypothesis, we observed a partial (~10-fold) loss of restriction in *Acod1*$^{-/-}$ BMMs

treated with the iNOS inhibitor 1400W, indicating that in the absence of IRG1, iNOS function is required to mediate full restriction of *L. pneumophila* in IFNγ-stimulated BMMs (**Figure 4C**). Reinforcing the idea that the activities of iNOS and IRG1 are redundant in terms of the IFNγ-coordinated response to *L. pneumophila*, we observed that targeting of both *Nos2* and *Acod1*, but not each factor independently, in iCas9 BMMs resulted in a marked loss of IFNγ-dependent restriction of *L. pneumophila* (**Figure 4D**). We next crossed *Nos2*$^{-/-}$ and *Acod1*$^{-/-}$ mice to derive littermate *Nos2*$^{-/-}$ *Acod1*$^{-/-}$ and *Nos2*$^{+/-}$*Acod1*$^{-/-}$ mice. We observed greater loss of IFNγ-dependent *L. pneumophila* restriction in *Nos2*$^{-/-}$*Acod1*$^{-/-}$ relative to *Nos2*$^{+/-}$*Acod1*$^{-/-}$ BMMs (**Figure 4E** and **4F**). In sum, these results indicate that the function of either iNOS or IRG1 must be intact to mediate full restriction of *L. pneumophila* replication in IFNγ-stimulated macrophages. This result suggests that activation of each of these factors by IFNγ is sufficient, individually, to mediate full restriction of *L. pneumophila*.

**BMMs deficient in six genes are fully defective in restriction *L. pneumophila* upon stimulation by IFNγ.** While it appears that iNOS and IRG1 are sufficient and redundant in coordinating a large proportion of *L. pneumophila* restriction in IFNγ-stimulated BMMs, we observed that BMMs deficient in both iNOS and IRG1 retain partial restriction of *L. pneumophila* replication (**Figure 4D – 4F**). In an effort to pinpoint the additional factors that mediate IFNγ-dependent restriction of *L. pneumophila* in BMMs, we made use of existing QKO mice lacking functional iNOS, NADPH oxidase 2 (NOX2), and immunity-related GTPase family M members 1 and 3 (IRGM1, IRGM3) (20). To test the hypothesis that the six factors implicated across our observations (iNOS, IRG1) and

the studies by Pilla *et al* (QKO, CASP11) and Naujoks *et al* (IRG1) comprise the entirety of the IFNγ-coordinated response to *L. pneumophila* in macrophages, we employed CRISPR/Cas9 to target *Casp11* and *Acod1* (**Table 1**) in QKO mouse embryos to generate three novel mouse strains: QKO mice that also lack functional CASP11 (QKO/C11), QKO mice that also lack functional IRG1 (QKO/IRG1), and QKO mice that additionally lack both CASP11 and IRG1 (6KO). As previously reported, and in line with our observations in *Nos2* single knockout BMMs, we observed that IFNγ-dependent restriction of *L. pneumophila* in QKO BMMs was largely intact, indicating that no gene disrupted in these cells is absolutely required for restriction of *L. pneumophila* (**Figure 5A** and **5B**). QKO/C11 BMMs did not lose IFNγ-mediated restriction relative to QKO BMMs (**Figure 5A** and **5B**). In contrast, we observed a striking loss of restriction in QKO/IRG1 BMMs and, effectively, a total loss of *L. pneumophila* restriction in 6KO BMMs stimulated with IFNγ (**Figure 5A** and **5B**).

If the ability of 2DG to rescue *L. pneumophila* in IFNγ-treated BMMs acts through inhibition of iNOS and IRG1, we would expect 2DG to have no effect in BMMs lacking expression of these factors. In fact, we observed that in comparison with QKO BMMs, 2DG retained the ability to partially rescue *L. pneumophila* replication in *Nos2*$^{-/-}$ *Acod1*$^{-/-}$ BMMs stimulated with IFNγ (**Figure 5C**). However, the rescue effect of 2DG was absent in QKO/IRG1 BMMs (**Figure 5C**). Transcript profiling did not reveal an inhibitory effect of 2DG on expression of the other genes disrupted in the QKO/IRG1 background (**Supplementary Figure 4B**). This result indicates that 2DG may mediate some beneficial metabolic effect for *L. pneumophila* independent of regulating activity of iNOS and IRG1; however, these effects may require the other factors disrupted in the QKO

background. Alternately, the potential metabolic effects of 2DG may be obscured by the profound loss of restriction observed in QKO/IRG1 BMMs.

In sum, these results further underscore our previous observation that iNOS and IRG1 are each sufficient in terms of mediating a large proportion of the IFNγ-dependent restriction of *L. pneumophila* in BMMs, as the addition of IRG1 deficiency to the QKO background profoundly disabled IFNγ-mediated restriction. Further, our data reveal a partial role for CASP11 in control of *L. pneumophila* restriction in IFNγ-stimulated BMMs, given the differences observed between QKO/IRG1 and 6KO BMMs. Finally, our results demonstrate that the six genes disrupted in 6KO BMMs, or a subset of those six that includes *Nos2*, *Acod1*, and *Casp11*, coordinate(s) the entirety of the IFNγ-dependent, cell-intrinsic control of *L. pneumophila* observed in BMMs.

## Discussion

Our results support a model in which IFNγ restricts *L. pneumophila* replication in mammalian macrophages through activation of multiple redundant factors including iNOS and IRG1. To date, no study has identified a macrophage deficient in any single IFNγ-stimulated gene that is impaired in the ability to restrict *L. pneumophila* replication when stimulated with IFNγ. Even QKO macrophages, which lack three other potentially antimicrobial factors in addition to iNOS, do not lose IFNγ-mediated restriction of *L. pneumophila*, reinforcing the notion that redundant mechanisms contribute to IFNγ-mediated bacterial control in macrophages.

Our recent identification of a strain of *L. pneumophila* resistant to the direct antimicrobial effect of 2DG when growing in BMMs (36) allowed us to test the

hypothesis that global disruption of macrophage metabolism would interfere with the antimicrobial effects of IFNγ. Indeed, 2DG partially reversed the restriction of *L. pneumophila* replication by IFNγ in BMMs. However, neither the glycolysis inhibition activity nor the UPR induction activity of 2DG, *per se*, appears to underlie the ability of this drug to subvert the antimicrobial effect of IFNγ. Instead, 2DG appears to regulate the IFNγ-dependent induction of iNOS and IRG1 via some as-yet unidentified mechanism. In addition, there appears to be some effect of 2DG independent of iNOS and IRG1 regulation, suggesting that metabolic perturbation could interfere with the antimicrobial activities of IFNγ in infected macrophages. Ultimately, experimentation with 2DG and other stimuli that reversed IFNγ-mediated restriction of *L. pneumophila* led us to the discovery that both iNOS and IRG1 appear to be fully sufficient, and therefore redundant, in terms of mediating IFNγ-coordinated immune response to *L. pneumophila* in macrophages.

A complex picture is emerging in terms of the role of IRG1 and the metabolite it produces, itaconate, during inflammation and infection. A direct antimicrobial role for itaconate via poisoning the bacterial glyoxylate pathway has been suggested for *Mtb* and *L. pneumophila* (21, 25). IRG1 was shown to be an essential component of the immune response to *Mtb*, as *Acod1*$^{-/-}$ mice succumbed more rapidly than wild-type to infection; however, IRG1 appeared to be required for regulation of non-cell-autonomous pathological inflammation, and there was no evidence for cell-intrinsic antimicrobial effects of itaconate (50). IRG1 has also been demonstrated to be protective in a model of Zika virus infection in neurons (51). Interestingly, other studies have demonstrated anti-inflammatory effects of itaconate on myeloid cells, suggesting it may act as part of a

353 negative feedback loop to control inflammation (27, 52). Beyond production of itaconate,
354 the disruption of oxidative metabolic pathways caused by IRG1 activity may promote
355 antimicrobial metabolic shifts in macrophages. Ultimately, diverse cell-intrinsic and
356 intercellular roles for IRG1 and itaconate likely contribute to the immune response to a
357 broad array of pathogens. Our data demonstrate that IRG1 is not required for the cell-
358 intrinsic immune response to *L. pneumophila* in macrophages treated with IFNγ, but
359 indeed may be sufficient to coordinate IFNγ-mediated restriction of *L. pneumophila,* as
360 previously reported (21). Both NO generated by iNOS and itaconate generated by IRG1
361 may be directly antimicrobial to *L. pneumophila* in macrophages stimulated with IFNγ.
362 Alternately or additionally, iNOS and IRG1 may act to restrict *L. pneumophila* replication
363 via coordinating global changes in macrophage metabolism that restrict access to key
364 bacterial metabolites or otherwise render the host macrophage inhospitable for bacterial
365 growth.

366 Adding *Acod1* and *Casp11* deficiency to the QKO background revealed further
367 layers of redundancy in the immune response to *L. pneumophila* coordinated by IFNγ.
368 While QKO/C11 macrophages did not differ meaningfully from QKO macrophages in
369 terms of IFNγ-mediated bacterial restriction, we observed a profound loss of restriction
370 in QKO/IRG1 macrophages, beyond what we observed in primary *Nos2*$^{-/-}$ *Acod1*$^{-/-}$
371 macrophages. This result indicates that factors other than iNOS disrupted in the QKO
372 background may play a role in limiting *L. pneumophila* in IFNγ-stimulated macrophages.

373 In agreement with the results of Pilla *et al* (20), our data suggest that a role exists
374 for CASP11 in the IFNγ-mediated immune response to *L. pneumophila*, given the near-
375 complete inability of IFNγ to restrict *L. pneumophila* replication in 6KO macrophages vs.

376 QKO/IRG macrophages (that retain CASP11). In combination with the data showing
377 that *Casp1/11*$^{-/-}$ and QKO/C11 BMMs retain IFNγ-mediated bacterial restriction, this
378 result demonstrates that the activity of CASP11 is also redundant, at least with the
379 activities of iNOS and IRG1.
380 In sum, our study reveals a more comprehensive picture of the factors that are
381 necessary and sufficient to coordinate the IFNγ-dependent immune response to *L.*
382 *pneumophila*. While we have not determined whether all six of the genes disrupted in
383 6KO BMMs cells are required to fully exert IFNγ-dependent cell-intrinsic restriction of *L.*
384 *pneumophila* or a subset of the six that includes iNOS, IRG1, and CASP11, we are
385 encouraged that among the numerous genes transcribed in IFNγ-stimulated
386 macrophages we have narrowed the field that mediate cell-intrinsic control of *L.*
387 *pneumophila* to six candidates. While all of the gene products disrupted in the 6KO
388 background could function directly as antimicrobial effectors, we also note the possibility
389 that some or all may function as upstream regulators and thus affect *L. pneumophila*
390 indirectly.
391 IFNγ is an essential component of the immune response to bacterial pathogens
392 beyond *L. pneumophila*. Thus, the implications of this study extend beyond furthering
393 our understanding of the immune response to *L. pneumophila*, an accidental pathogen
394 of mammals that did not evolve to evade the human immune response. Our work
395 reveals fundamental redundancy in the IFNγ-dependent immune response to potentially
396 pathogenic environmental microbes. Dissecting these overlapping innate immune
397 strategies reveals the complexity and comprehensiveness of the innate immune barrier
398 posed to novel environmental microorganisms by mammalian macrophages and IFNγ.

399 Further, a more detailed understanding of how IFNγ can mediate bacterial restriction in
400 host cells may inform studies of how "professional" pathogens, such as *Mtb*, *S. enterica*,
401 and *L. monocytogenes*, have evolved to avoid or subvert these effects of IFNγ.
402
403 **Materials and Methods**
404 **Ethics statement.** We conducted experiments in this study according to guidelines
405 established by the *Guide for the Care and Use of Laboratory Animals* of the National
406 Institutes of Health (53) under a protocol approved by the Animal Care and Use
407 Committee at the University of California, Berkeley (AUP-2014-09-6665).
408
409 **Bone marrow-derived macrophages.** We purchased wild-type C57BL/6 (strain
410 000664), *Ifngr*$^{-/-}$ (strain 003288), *Ifnar*$^{-/-}$ (strain 028288), *Myd88*$^{-/-}$ (strain 009088),
411 *Nos2*$^{-/-}$ (strain 002609), *Acod1*$^{-/-}$ (strain 029340), and C57BL/6N (strain 005304) mice
412 from Jackson Laboratory as a source of bone marrow to derive macrophages.
413 *Casp1/11*$^{-/-}$ mice were provided by A. Van der Velden and M. Starnbach (54). *Myd88*$^{-/-}$
414 *Nod1*$^{-/-}$ *Nod2*$^{-/-}$ mice were generated at UC Berkeley as described previously (39).
415 *Nos2*$^{-/-}$*Irg1*$^{-/-}$, and *Nos2*$^{+/-}$*Irg1*$^{-/-}$ mice were also generated by crossing in-house at UC
416 Berkeley. QKO mice (*Nos2*$^{-/-}$, *Cybb*$^{-/-}$, *Irgm1*$^{-/-}$, *Irgm3*$^{-/-}$), generously provided by the
417 lab of Christopher Sassetti at the University of Massachusetts, and mice lacking a
418 section of chromosome 3 containing GBPs 1, 2, 3, 5, and 7 (*Gbp*$^{chr3-/-}$) and wild-type
419 control mice (*Gbp*$^{chr3+/+}$), all on the C57BL/6 background were generated as described
420 (20). We derived bone marrow-derived macrophages (BMMs) in RPMI supplemented

421 with 10% fetal bovine serum, 2.0 mM L-glutamine, 100 µM streptomycin (all from Life
422 Technologies), and 5% supernatant from 3T3 cells expressing macrophage colony-
423 stimulating factor (generated in-house). Macrophages derived from LysMCre$^{+/+}$ and
424 LysMCre$^{+/+}$*Atg5*$^{fl/fl}$ mice on the C57BL/6 background were provided by Daniel Portnoy
425 and Jeffery Cox at UC Berkeley. Macrophages derived from LysMCre$^{+/+}$ and
426 LysMCre$^{+/+}$*Hif1a*$^{fl/fl}$ mice on the C57BL/6 background were provided by Sarah Stanley
427 at UC Berkeley.
428
429 **Mouse CRISPR**. We generated QKO/C11 and QKO/IRG1 mice by pronuclear injection
430 of Cas9 mRNA and guide RNAs into fertilized embryos of QKO mice as described
431 previously (55). Founder male mice heterozygous for mutation in either *Casp11* or
432 *Acod1* were backcrossed once onto the QKO background and offspring were
433 intercrossed to generate QKO/C11, QKO/IRG1, and 6KO mice. *Acod1* mutation was
434 determined by amplifying a fragment of genomic DNA surrounding the cut site targeted
435 in *Acod1* exon 2 (forward primer: AACTCTGGGAATGCCAGCTC, reverse primer:
436 GGAGCCACAACAGGGATCAA, yielding a ~440 base-pair PCR product) and Sanger
437 sequencing, which revealed a three-nucleotide deletion (TTC) and a one-nucleotide
438 insertion (A) at the cut site in mutant DNA resulting in a frame-shift mutation and
439 premature stop codon. *Casp11* mutation was determined by amplifying genomic DNA
440 surrounding the cut sites indicated by both guide RNAs (forward primer:
441 GGGGCTCTGAAAAGGTGTGA, reverse primer: TCTAGACACAAAGCCCATGT,
442 revealing a ~520-base pair band in wild-type DNA and a ~290-base pair band in mutant
443 DNA, indicating a missing ~230-base pair fragment in mutant genomic DNA.

444

445 **iCas9 CRISPR**. We cloned template DNA for the indicated guide RNAs into a pLX-
446 sgRNA construct additionally containing blasticidin resistance (Addgene plasmid
447 #50662). We transfected constructs into HEK293T cells along with lentivirus packaging
448 vector pSPAX2 (Addgene plasmid #12260) and lentivirus envelope vector VSV-G
449 (Addgene plasmid #8454). We used the resulting virus particles to transduce
450 immortalized wild-type C57BL/6 cells that express doxycycline-inducible SpCas9
451 enzyme (generated using Addgene plasmid #50661). We cultured transduced cells in
452 3.0 μg/ml blasticidin (Invivogen) and 5.0 μg/ml doxycycline (Sigma) for at least two
453 weeks prior to use in experiments.

454

455 **Bacterial strains, infection and stimulation of BMMs.** LP02 is a thymidine auxotroph
456 derived from LP01, a clinical isolate of *L. pneumophila* (56). Generation of Δ*flaA* and
457 luminescent strains of *L. pneumophila* have been described previously (36, 37). We
458 cultured all strains of *L. pneumophila* in AYE (ACES-buffered yeast extract broth) or on
459 ACES-buffered charcoal-yeast extract (BCYE) agar plates at 37 °C. For measurement
460 of intracellular *L. pneumophila* growth by luminescence or by CFU, we plated 100k
461 BMMs/well in opaque white TC-treated 96-well microtiter plates and infected with *L.*
462 *pneumophila* at a multiplicity of infection of 0.05. One hour post-infection by
463 centrifugation at 287 × *g*, we replaced the media of infected BMMs with media ±
464 stimulation at indicated concentrations. At the indicated times following infection, we
465 measured bacterial growth by detection of luminescence at λ = 470 using a Spectramax
466 L luminometer (Bio-Rad) or by dilution of infected cultures on BYCE agar plates for

enumeration of CFU. Pam3CSK4 and *E. coli*-derived LPS were purchased from Invivogen. As indicated, we added recombinant mouse IFNγ (ThermoFisher), 2-deoxyglucose (Abcam), brefeldin A (BD), 1400W (Cayman Chemical), 3-bromopyruvte, sodium oxamate, galactose, geldanamycin, dithiothreitol, tunicamycin, thapsigargin, and ISRIB (all from Sigma). We performed lactate and glucose measurement with kits purchased from Sigma according to manufacturer instructions.

**Western Blot.** Following stimulation for 24 hours, we mixed lysates derived from 1.0 x $10^6$ BMMs per stimulation condition with SDS sample buffer (40% glycerol, 8% SDS, 2% 2-mercaptoethanol, 40 mM EDTA, 0.05% bromophenol blue and 250 mM Tris-HCl, pH 6.8), boiled for 5 min and then separated by SDS-PAGE. Rabbit Anti-IRG1 antibody was from Abcam (ab222417) and mouse anti-β actin antibody was from Santa Cruz (47778).

**RNAseq.** We submitted RNA purified from the indicated cell culture conditions using an RNeasy kit (Qiagen) to the QB3-Berkeley Functional Genomics Laboratory, where single-read 100 base pair read length (SR100) sequencing libraries were generated. Libraries were sequenced using either a HiSeq2500 System (Illumina) at the New York Genome Center (New York, NY) or a HiSeq4000 System (Illumina) at the Vincent J. Coates Genomics Sequencing Laboratory at UC Berkeley. We performed alignment, differential expression analysis, and gene set enrichment as described previously (57-59).

**Data Availability.** We deposited the RNAseq data associated with this study in the NCBI Gene Expression Omnibus, available at https://www.ncbi.nlm.nih.gov/geo/ via accession numbers GSE135385 and GSE135386.

**Acknowledgements**

R.E.V. is supported by an Investigator Award from the Howard Hughes Medical Institute and by NIH grants AI063302 and AI075039. We would like to thank Harmandeep Dhaliwal at the Cancer Research Laboratory Gene Targeting Facility at UC Berkeley for assistance in generating mouse strains used in this study. We would also like to thank Kevin Barry for assistance with RNAseq analysis. We acknowledge stimulating discussions with Sarah Stanley, Jonathan Braverman, Greg Barton, Daniel Portnoy, and members of the Vance, Stanley, Barton, and Portnoy Labs, and members of the P01 Intracellular Pathogens and Innate Immunity research group. The authors have no conflicts of interest with regard to the results presented in this study.

## References


1. Price JV, Vance RE. 2014. The macrophage paradox. Immunity 41:685-93.
2. Bustamante J, Boisson-Dupuis S, Abel L, Casanova JL. 2014. Mendelian susceptibility to mycobacterial disease: genetic, immunological, and clinical features of inborn errors of IFN-gamma immunity. Semin Immunol 26:454-70.
3. Cooper AM, Dalton DK, Stewart TA, Griffin JP, Russell DG, Orme IM. 1993. Disseminated tuberculosis in interferon gamma gene-disrupted mice. J Exp Med 178:2243-7.
4. Flynn JL, Chan J, Triebold KJ, Dalton DK, Stewart TA, Bloom BR. 1993. An essential role for interferon gamma in resistance to Mycobacterium tuberculosis infection. J Exp Med 178:2249-54.
5. Harty JT, Bevan MJ. 1995. Specific immunity to Listeria monocytogenes in the absence of IFN gamma. Immunity 3:109-17.
6. Bao S, Beagley KW, France MP, Shen J, Husband AJ. 2000. Interferon-gamma plays a critical role in intestinal immunity against Salmonella typhimurium infection. Immunology 99:464-72.
7. Murphy EA, Sathiyaseelan J, Parent MA, Zou B, Baldwin CL. 2001. Interferon-gamma is crucial for surviving a Brucella abortus infection in both resistant C57BL/6 and susceptible BALB/c mice. Immunology 103:511-8.
8. Shinozawa Y, Matsumoto T, Uchida K, Tsujimoto S, Iwakura Y, Yamaguchi K. 2002. Role of interferon-gamma in inflammatory responses in murine respiratory infection with Legionella pneumophila. J Med Microbiol 51:225-30.

525 9. Archer KA, Alexopoulou L, Flavell RA, Roy CR. 2009. Multiple MyD88-dependent
526 responses contribute to pulmonary clearance of Legionella pneumophila. Cell
527 Microbiol 11:21-36.
528 10. Brown AS, Yang C, Fung KY, Bachem A, Bourges D, Bedoui S, Hartland EL, van
529 Driel IR. 2016. Cooperation between Monocyte-Derived Cells and Lymphoid
530 Cells in the Acute Response to a Bacterial Lung Pathogen. PLoS Pathog
531 12:e1005691.
532 11. MacMicking JD, North RJ, LaCourse R, Mudgett JS, Shah SK, Nathan CF. 1997.
533 Identification of nitric oxide synthase as a protective locus against tuberculosis.
534 Proc Natl Acad Sci U S A 94:5243-8.
535 12. Khan IA, Schwartzman JD, Matsuura T, Kasper LH. 1997. A dichotomous role for
536 nitric oxide during acute Toxoplasma gondii infection in mice. Proc Natl Acad Sci
537 U S A 94:13955-60.
538 13. Chakravortty D, Hensel M. 2003. Inducible nitric oxide synthase and control of
539 intracellular bacterial pathogens. Microbes Infect 5:621-7.
540 14. Braverman J, Sogi KM, Benjamin D, Nomura DK, Stanley SA. 2016. HIF-1alpha
541 Is an Essential Mediator of IFN-gamma-Dependent Immunity to Mycobacterium
542 tuberculosis. J Immunol 197:1287-97.
543 15. Braverman J, Stanley SA. 2017. Nitric Oxide Modulates Macrophage Responses
544 to Mycobacterium tuberculosis Infection through Activation of HIF-1alpha and
545 Repression of NF-kappaB. J Immunol 199:1805-1816.
546 16. Mishra BB, Rathinam VA, Martens GW, Martinot AJ, Kornfeld H, Fitzgerald KA,
547 Sassetti CM. 2013. Nitric oxide controls the immunopathology of tuberculosis by

548 inhibiting NLRP3 inflammasome-dependent processing of IL-1beta. Nat Immunol
549 14:52-60.
550 17. Mishra BB, Lovewell RR, Olive AJ, Zhang G, Wang W, Eugenin E, Smith CM,
551 Phuah JY, Long JE, Dubuke ML, Palace SG, Goguen JD, Baker RE, Nambi S,
552 Mishra R, Booty MG, Baer CE, Shaffer SA, Dartois V, McCormick BA, Chen X,
553 Sassetti CM. 2017. Nitric oxide prevents a pathogen-permissive granulocytic
554 inflammation during tuberculosis. Nat Microbiol 2:17072.
555 18. Nathan C. 1997. Inducible nitric oxide synthase: what difference does it make? J
556 Clin Invest 100:2417-23.
557 19. Summersgill JT, Powell LA, Buster BL, Miller RD, Ramirez JA. 1992. Killing of
558 Legionella pneumophila by nitric oxide in gamma-interferon-activated
559 macrophages. J Leukoc Biol 52:625-9.
560 20. Pilla DM, Hagar JA, Haldar AK, Mason AK, Degrandi D, Pfeffer K, Ernst RK,
561 Yamamoto M, Miao EA, Coers J. 2014. Guanylate binding proteins promote
562 caspase-11-dependent pyroptosis in response to cytoplasmic LPS. Proc Natl
563 Acad Sci U S A 111:6046-51.
564 21. Naujoks J, Tabeling C, Dill BD, Hoffmann C, Brown AS, Kunze M, Kempa S,
565 Peter A, Mollenkopf HJ, Dorhoi A, Kershaw O, Gruber AD, Sander LE,
566 Witzenrath M, Herold S, Nerlich A, Hocke AC, van Driel I, Suttorp N, Bedoui S,
567 Hilbi H, Trost M, Opitz B. 2016. IFNs Modify the Proteome of Legionella-
568 Containing Vacuoles and Restrict Infection Via IRG1-Derived Itaconic Acid. PLoS
569 Pathog 12:e1005408.

570 22. Ellis TN, Beaman BL. 2004. Interferon-gamma activation of polymorphonuclear
571 neutrophil function. Immunology 112:2-12.
572 23. Casbon AJ, Long ME, Dunn KW, Allen LA, Dinauer MC. 2012. Effects of IFN-
573 gamma on intracellular trafficking and activity of macrophage NADPH oxidase
574 flavocytochrome b558. J Leukoc Biol 92:869-82.
575 24. Lippmann J, Muller HC, Naujoks J, Tabeling C, Shin S, Witzenrath M, Hellwig K,
576 Kirschning CJ, Taylor GA, Barchet W, Bauer S, Suttorp N, Roy CR, Opitz B.
577 2011. Dissection of a type I interferon pathway in controlling bacterial intracellular
578 infection in mice. Cell Microbiol 13:1668-82.
579 25. Michelucci A, Cordes T, Ghelfi J, Pailot A, Reiling N, Goldmann O, Binz T,
580 Wegner A, Tallam A, Rausell A, Buttini M, Linster CL, Medina E, Balling R, Hiller
581 K. 2013. Immune-responsive gene 1 protein links metabolism to immunity by
582 catalyzing itaconic acid production. Proc Natl Acad Sci U S A 110:7820-5.
583 26. Lampropoulou V, Sergushichev A, Bambouskova M, Nair S, Vincent EE,
584 Loginicheva E, Cervantes-Barragan L, Ma X, Huang SC, Griss T, Weinheimer
585 CJ, Khader S, Randolph GJ, Pearce EJ, Jones RG, Diwan A, Diamond MS,
586 Artyomov MN. 2016. Itaconate Links Inhibition of Succinate Dehydrogenase with
587 Macrophage Metabolic Remodeling and Regulation of Inflammation. Cell Metab
588 24:158-66.
589 27. Hooftman A, O'Neill LAJ. 2019. The Immunomodulatory Potential of the
590 Metabolite Itaconate. Trends Immunol doi:10.1016/j.it.2019.05.007.
591 28. Ensminger AW, Isberg RR. 2009. Legionella pneumophila Dot/Icm translocated
592 substrates: a sum of parts. Curr Opin Microbiol 12:67-73.

593 29. Molofsky AB, Byrne BG, Whitfield NN, Madigan CA, Fuse ET, Tateda K,
594 Swanson MS. 2006. Cytosolic recognition of flagellin by mouse macrophages
595 restricts Legionella pneumophila infection. J Exp Med 203:1093-104.
596 30. Ren T, Zamboni DS, Roy CR, Dietrich WF, Vance RE. 2006. Flagellin-deficient
597 Legionella mutants evade caspase-1- and Naip5-mediated macrophage
598 immunity. PLoS Pathog 2:e18.
599 31. Lightfield KL, Persson J, Brubaker SW, Witte CE, von Moltke J, Dunipace EA,
600 Henry T, Sun YH, Cado D, Dietrich WF, Monack DM, Tsolis RM, Vance RE.
601 2008. Critical function for Naip5 in inflammasome activation by a conserved
602 carboxy-terminal domain of flagellin. Nat Immunol 9:1171-8.
603 32. Zamboni DS, Kobayashi KS, Kohlsdorf T, Ogura Y, Long EM, Vance RE, Kuida
604 K, Mariathasan S, Dixit VM, Flavell RA, Dietrich WF, Roy CR. 2006. The Birc1e
605 cytosolic pattern-recognition receptor contributes to the detection and control of
606 Legionella pneumophila infection. Nat Immunol 7:318-25.
607 33. Amer A, Franchi L, Kanneganti TD, Body-Malapel M, Ozoren N, Brady G,
608 Meshinchi S, Jagirdar R, Gewirtz A, Akira S, Nunez G. 2006. Regulation of
609 Legionella phagosome maturation and infection through flagellin and host Ipaf. J
610 Biol Chem 281:35217-23.
611 34. Wright EK, Goodart SA, Growney JD, Hadinoto V, Endrizzi MG, Long EM,
612 Sadigh K, Abney AL, Bernstein-Hanley I, Dietrich WF. 2003. Naip5 affects host
613 susceptibility to the intracellular pathogen Legionella pneumophila. Curr Biol
614 13:27-36.

615 35. Diez E, Lee SH, Gauthier S, Yaraghi Z, Tremblay M, Vidal S, Gros P. 2003.
616 Birc1e is the gene within the Lgn1 locus associated with resistance to Legionella
617 pneumophila. Nat Genet 33:55-60.
618 36. Price JV, Jiang K, Galantowicz A, Freifeld A, Vance RE. 2018. Legionella
619 pneumophila Is Directly Sensitive to 2-Deoxyglucose-Phosphate via Its UhpC
620 Transporter but Is Indifferent to Shifts in Host Cell Glycolytic Metabolism. J
621 Bacteriol 200.
622 37. Coers J, Vance RE, Fontana MF, Dietrich WF. 2007. Restriction of Legionella
623 pneumophila growth in macrophages requires the concerted action of cytokine
624 and Naip5/Ipaf signalling pathways. Cell Microbiol 9:2344-57.
625 38. Goncalves AV, Margolis SR, Quirino GFS, Mascarenhas DPA, Rauch I, Nichols
626 RD, Ansaldo E, Fontana MF, Vance RE, Zamboni DS. 2019. Gasdermin-D and
627 Caspase-7 are the key Caspase-1/8 substrates downstream of the
628 NAIP5/NLRC4 inflammasome required for restriction of Legionella pneumophila.
629 PLoS Pathog 15:e1007886.
630 39. Fontana MF, Shin S, Vance RE. 2012. Activation of host mitogen-activated
631 protein kinases by secreted Legionella pneumophila effectors that inhibit host
632 protein translation. Infect Immun 80:3570-5.
633 40. Yang Z, Klionsky DJ. 2010. Mammalian autophagy: core molecular machinery
634 and signaling regulation. Curr Opin Cell Biol 22:124-31.
635 41. Sauer JD, Sotelo-Troha K, von Moltke J, Monroe KM, Rae CS, Brubaker SW,
636 Hyodo M, Hayakawa Y, Woodward JJ, Portnoy DA, Vance RE. 2011. The N-
637 ethyl-N-nitrosourea-induced Goldenticket mouse mutant reveals an essential

function of Sting in the in vivo interferon response to Listeria monocytogenes and cyclic dinucleotides. Infect Immun 79:688-94.

42. Escoll P, Song OR, Viana F, Steiner B, Lagache T, Olivo-Marin JC, Impens F, Brodin P, Hilbi H, Buchrieser C. 2017. Legionella pneumophila Modulates Mitochondrial Dynamics to Trigger Metabolic Repurposing of Infected Macrophages. Cell Host Microbe 22:302-316 e7.

43. Warren WJ, Miller RD. 1979. Growth of Legionnaires disease bacterium (Legionella pneumophila) in chemically defined medium. J Clin Microbiol 10:50-5.

44. Tesh MJ, Morse SA, Miller RD. 1983. Intermediary metabolism in Legionella pneumophila: utilization of amino acids and other compounds as energy sources. J Bacteriol 154:1104-9.

45. Eylert E, Herrmann V, Jules M, Gillmaier N, Lautner M, Buchrieser C, Eisenreich W, Heuner K. 2010. Isotopologue profiling of Legionella pneumophila: role of serine and glucose as carbon substrates. J Biol Chem 285:22232-43.

46. Rossignol R, Gilkerson R, Aggeler R, Yamagata K, Remington SJ, Capaldi RA. 2004. Energy substrate modulates mitochondrial structure and oxidative capacity in cancer cells. Cancer Res 64:985-93.

47. Gaddameedhi S, Chatterjee S. 2009. Association between the unfolded protein response, induced by 2-deoxyglucose, and hypersensitivity to cisplatin: a mechanistic study employing molecular genomics. J Cancer Res Ther 5 Suppl 1:S61-6.

48. Sidrauski C, Acosta-Alvear D, Khoutorsky A, Vedantham P, Hearn BR, Li H, Gamache K, Gallagher CM, Ang KK, Wilson C, Okreglak V, Ashkenazi A, Hann

B, Nader K, Arkin MR, Renslo AR, Sonenberg N, Walter P. 2013. Pharmacological brake-release of mRNA translation enhances cognitive memory. Elife 2:e00498.

49. Pakos-Zebrucka K, Koryga I, Mnich K, Ljujic M, Samali A, Gorman AM. 2016. The integrated stress response. EMBO Rep 17:1374-1395.

50. Nair S, Huynh JP, Lampropoulou V, Loginicheva E, Esaulova E, Gounder AP, Boon ACM, Schwarzkopf EA, Bradstreet TR, Edelson BT, Artyomov MN, Stallings CL, Diamond MS. 2018. Irg1 expression in myeloid cells prevents immunopathology during M. tuberculosis infection. J Exp Med 215:1035-1045.

51. Daniels BP, Kofman SB, Smith JR, Norris GT, Snyder AG, Kolb JP, Gao X, Locasale JW, Martinez J, Gale M, Jr., Loo YM, Oberst A. 2019. The Nucleotide Sensor ZBP1 and Kinase RIPK3 Induce the Enzyme IRG1 to Promote an Antiviral Metabolic State in Neurons. Immunity 50:64-76 e4.

52. Mills EL, Ryan DG, Prag HA, Dikovskaya D, Menon D, Zaslona Z, Jedrychowski MP, Costa ASH, Higgins M, Hams E, Szpyt J, Runtsch MC, King MS, McGouran JF, Fischer R, Kessler BM, McGettrick AF, Hughes MM, Carroll RG, Booty LM, Knatko EV, Meakin PJ, Ashford MLJ, Modis LK, Brunori G, Sevin DC, Fallon PG, Caldwell ST, Kunji ERS, Chouchani ET, Frezza C, Dinkova-Kostova AT, Hartley RC, Murphy MP, O'Neill LA. 2018. Itaconate is an anti-inflammatory metabolite that activates Nrf2 via alkylation of KEAP1. Nature 556:113-117.

53. (ed). 2011. Guide for the care and use of laboratory animals. National Academies Press,, Washington, D.C. http://www.ncbi.nlm.nih.gov/books/NBK54050 ebrary http://site.ebrary.com/id/10443276

National Academies Press http://www.nap.edu/catalog.php?record_id=12910

National Academies Press http://www.nap.edu/catalog.php?record_id=12910 - toc

http://www.ncbi.nlm.nih.gov/bookshelf/br.fcgi?book=nap12910

http://grants.nih.gov/grants/olaw/Guide-for-the-Care-and-use-of-laboratory-animals.pdf. Accessed

54. Li P, Allen H, Banerjee S, Franklin S, Herzog L, Johnston C, McDowell J, Paskind M, Rodman L, Salfeld J, et al. 1995. Mice deficient in IL-1 beta-converting enzyme are defective in production of mature IL-1 beta and resistant to endotoxic shock. Cell 80:401-11.

55. Wang H, Yang H, Shivalila CS, Dawlaty MM, Cheng AW, Zhang F, Jaenisch R. 2013. One-step generation of mice carrying mutations in multiple genes by CRISPR/Cas-mediated genome engineering. Cell 153:910-8.

56. Berger KH, Isberg RR. 1993. Two distinct defects in intracellular growth complemented by a single genetic locus in Legionella pneumophila. Mol Microbiol 7:7-19.

57. Trapnell C, Roberts A, Goff L, Pertea G, Kim D, Kelley DR, Pimentel H, Salzberg SL, Rinn JL, Pachter L. 2012. Differential gene and transcript expression analysis of RNA-seq experiments with TopHat and Cufflinks. Nat Protoc 7:562-78.

58. Bray NL, Pimentel H, Melsted P, Pachter L. 2016. Near-optimal probabilistic RNA-seq quantification. Nat Biotechnol 34:525-7.

59. Zhou Y, Zhou B, Pache L, Chang M, Khodabakhshi AH, Tanaseichuk O, Benner C, Chanda SK. 2019. Metascape provides a biologist-oriented resource for the analysis of systems-level datasets. Nat Commun 10:1523.

## Figure Legends.

**Figure 1. IFNγ restricts *L. pneumophila* replication across a spectrum of immune response-impaired macrophage genotypes.** (**A**) Luminescence measured in relative light units (RLU, left) and recovery of colony forming units (CFU, right) of LP02 Δ*flaA* lux *L. pneumophila* from infected wild-type C57BL/6 BMMs either not stimulated (no stim) or stimulated with 6.0 ng/mL IFNγ. (**B**) RLU from LP02 Δ*flaA* lux *L. pneumophila* from infected *Ifngr*$^{-/-}$ and *Nos2*$^{-/-}$ BMMs either not stimulated or stimulated with 6.0 ng/mL IFNγ. (**C**) RLU from LP02 Δ*flaA* lux *L. pneumophila* from infected *Myd88*$^{-/-}$ and *Myd88*$^{-/-}$ *Nod1*$^{-/-}$ *Nod2*$^{-/-}$BMMs either not stimulated or stimulated with 6.0 ng/mL IFNγ. (**D**) RLU from LP02 Δ*flaA* lux *L. pneumophila* from infected LysMCre$^{+}$ *Atg5*$^{fl/fl}$ and LysMCre$^{+}$ BMMs either not stimulated or stimulated with 6.0 ng/mL IFNγ. (**E**) RLU from LP02 Δ*flaA* lux *L. pneumophila* from infected *Gbp*$^{chr3\ -/-}$, *Gbp*$^{chr3\ +/+}$, and *Casp1/11*$^{-/-}$ BMMs either unstimulated or stimulated with 6.0 ng/mL IFNγ. Data reflect individual experiments that represent at least two independent experiments. Error bars in all graphs represent standard deviation of the mean of at least three technical replicates. $p < 0.001$ comparing no stim vs. IFNγ curves in all genotypes of BMMs (except *Ifngr*$^{-/-}$) by 2-way ANOVA. No stim and IFNγ curves do not differ significantly in *Ifngr*$^{-/-}$ BMMs.

**Figure 2. 2DG rescues *L. pneumophila* replication in IFNγ-stimulated macrophages.** (**A**) RLU (left) and CFU (right) of LP02 Δ*flaA*Δ*uhpC* lux *L. pneumophila* from infected WT C57BL/6 BMMs either not stimulated (no stim), stimulated with 6.0

729 ng/mL IFNγ (IFNγ), or stimulated with 6.0 ng/mL IFNγ + 2.0 mM 2DG (IFNγ/2DG). $p <$
730 0.001 comparing all curves to each other in each graph by 2-way ANOVA. (**B**) Lactate
731 secretion (left) and glucose consumption (right) measured in cell culture media following
732 infection of WT C57BL/6 BMMs with LP02 Δ*flaA*Δ*uhpC* lux *L. pneumophila* and
733 stimulated with 6.0 ng/mL IFNγ and 1.0 mM 2DG as indicated. ** = $p < 0.01$; * = $p <$
734 0.05; ns = not significant comparing indicated curves by 2-way ANOVA. (**C**) RLU from
735 LP02 Δ*flaA*Δ*uhpC* lux *L. pneumophila* from infected LysMCre$^{+}$ *Hif1a*$^{fl/fl}$ and LysMCre$^{+}$
736 BMMs not stimulated or stimulated with 6.0 ng/mL IFNγ and 2.0 mM 2DG as indicated.
737 $p < 0.01$ comparing all curves to each other corresponding to each genotype by 2-way
738 ANOVA. (**D**) RLU from LP02 Δ*flaA*Δ*uhpC* lux *L. pneumophila* from infected WT
739 C57BL/6 BMMs stimulated with 6.0 ng/mL IFNγ and 2.0 mM 2DG as indicated and
740 cultured in infection media containing 11.11 mM glucose (left), 11.11 mM galactose in
741 the absence of glucose (center), and in glucose-free media with no exogenous source
742 of sugar (right). $p < 0.001$ comparing all curves to each other in each graph by 2-way
743 ANOVA. Data reflect results of individual experiments that represent at least three
744 independent experiments. Error bars in all graphs represent standard deviation of the
745 mean of at least three technical replicates.
746
747 **Figure 3. Differential effect of UPR stress stimuli on rescue of *L. pneumophila***
748 **replication in IFNγ-stimulated macrophages.** (**A**) RLU from LP02 Δ*flaA*Δ*uhpC* lux *L.*
749 *pneumophila* from infected WT C57BL/6 BMMs stimulated for 48 hours post-infection
750 with 6.0 ng/mL IFNγ, 2.0 mM 2DG, 2.0 μM geldanamycin (geld.), 1.0 μg/ml brefeldin A
751 (BfA), and 2.0 mM dithiothreitol (DTT) as indicated. (**B**) RLU from LP02 Δ*flaA*Δ*uhpC* lux

752 *L. pneumophila* from infected WT C57BL/6 BMMs stimulated for 48 hours post-infection
753 with 6.0 ng/mL IFNγ, 10.0 μM tunicamycin (tunic.), and 25.0 nM thapsigargin (thaps.) as
754 indicated. (**C**) RLU from LP02 Δ*flaA*Δ*uhpC* lux *L. pneumophila* from infected WT
755 C57BL/6 BMMs stimulated for 48 hours post-infection with 6.0 ng/mL IFNγ, 2.0 mM
756 2DG, 2.0 μM geldanamycin, and 0.1 μM ISRIB as indicated. *** = $p < 0.001$; ** = $p <$
757 0.01; * = $p < 0.05$; ns = not significant comparing means by unpaired *t* test. Data reflect
758 results of individual experiments that represent at least three independent experiments.
759 Error bars in all graphs represent standard deviation of the mean of at least two
760 technical replicates. Concentrations of UPR stimuli displayed represent a single point in
761 a titration at which we observed maximum effect on *L. pneumophila* replication in
762 combination with IFNγ stimulation relative to a minimum effect on *L. pneumophila*
763 replication in the absence of IFNγ.
764
765 **Figure 4. BMMs lacking IRG1 retain IFNγ-mediated restriction of *L. pneumophila***
766 **while BMMs lacking both INOS and IRG1 lose the ability to fully restrict *L.***
767 ***pneumophila*.** (**A**) RLU from LP02 Δ*flaA* lux *L. pneumophila* from infected iCas9 BMMs
768 in which *Acod1* was targeted with two guide RNAs (iCas9::*Acod1*), *Ifngr* was targeted
769 with one guide RNA (iCas9::*Ifngr*), or that were not manipulated (iCas9) not stimulated
770 (no stim) or stimulated with 6.0 ng/mL IFNγ. (**B**) RLU from LP02 Δ*flaA* lux *L.*
771 *pneumophila* from infected primary *Acod1*$^{-/-}$, and wild-type C57BL/6N BMMs not
772 stimulated or stimulated with 6.0 ng/mL IFNγ. C57BL/6N BMMs were included as a wild-
773 type control for BMMs derived from *Acod1*$^{-/-}$ mice, which were generated on the
774 C57BL/6N background. (**C**) RLU from LP02 Δ*flaA* lux *L. pneumophila* from infected

775 *Acod1*$^{-/-}$ and WT (C57BL/6N) BMMs either not stimulated (no stim), stimulated with 6.0
776 ng/mL IFNγ, or stimulated with 6.0 ng/mL IFNγ + 100 μM 1400W (IFNγ/1400W). p <
777 0.001 comparing no stim vs. IFNγ curves in both genotypes by 2-way ANOVA. IFNγ
778 does not differ significantly from IFNγ+1400W in C57BL/6N BMMs. (**D**) RLU from LP02
779 Δ*flaA* lux *L. pneumophila* from infected iCas9 BMMs in which *Nos2* was targeted with
780 two guide RNAs (iCas9::*Nos2*), *Acod1* was targeted with two guide RNAs
781 (iCas9::*Acod1*), both *Nos2* and *Acod1* were targeted with two guide RNAs each
782 (iCas9::*Nos2Acod1*), or that were not manipulated (iCas9) either not stimulated (no
783 stim) or stimulated with 6.0 ng/mL IFNγ. (**E**) RLU from LP02 Δ*flaA* lux *L. pneumophila*
784 from infected primary BMMs derived from *Nos2*$^{-/-}$*Acod1*$^{-/-}$ and littermate *Nos2*$^{+/-}$
785 *Acod1*$^{-/-}$ mice either not stimulated (no stim) or stimulated with 6.0 ng/mL IFNγ. *A* – *E*:
786 *** = p < 0.001; ** = p < 0.01; * = p < 0.05; ns = not significant comparing indicated
787 curves by 2-way ANOVA. (**F**) LP02 Δ*flaA* lux *L. pneumophila* CFU enumerated 48 hours
788 post-infection in BMMs derived from *Nos2*$^{-/-}$*Acod1*$^{-/-}$ and littermate *Nos2*$^{+/-}$*Acod1*$^{-/-}$
789 mice either not stimulated (no stim) or stimulated with 6.0 ng/mL IFNγ. ** = p < 0.01; * =
790 p < 0.05; ns = not significant comparing means by unpaired *t* test. Data reflect results of
791 individual experiments that represent at least two independent experiments. Error bars
792 in all graphs represent standard deviation of the mean of at least three technical
793 replicates.
794
795 **Figure 5. QKO BMMs that additionally lack functional either CASP11 and IRG1 or**
796 **both factors display partial to full lack of restriction of *L. pneumophila* replication**
797 **when stimulated with IFNγ.** (**A**) RLU from LP02 Δ*flaA* lux *L. pneumophila* from

infected C57BL/6, QKO, QKO/C11, QKO/IRG1, and 6KO BMMs either not stimulated (no stim) or stimulated with 6.0 ng/mL IFNγ. *** = $p < 0.001$; * = $p < 0.05$ comparing indicated curves by 2-way ANOVA. (**B**) CFU recovered from WT, QKO, QKO/C11, QKO/IRG1, and 6KO BMMs 48 hours following infection with LP02 Δ*flaA* lux *L. pneumophila*. **; = $p < 0.01$; * = $p < 0.05$; ns = not significant comparing means by unpaired *t* test. (**C**) RLU from LP02 Δ*flaA*Δ*uhpC* lux *L. pneumophila* from infected QKO, *Nos2*$^{-/-}$*Acod1*$^{-/-}$, and QKO/IRG1 BMMs stimulated with 6.0 ng/mL IFNγ and 2.0 mM 2DG as indicated. *** = $p < 0.001$**; ns = not significant comparing indicated curves by 2-way ANOVA. Data reflect results of individual experiments that represent at least three independent experiments. Error bars in all graphs represent standard deviation of the mean of at least three technical replicates.

**Supplementary Figure 1. 3-bromopyruvate and sodium oxamate do not rescue Δ*flaA*Δ*uhpC L. pneumophila* replication in IFNγ-stimulated BMMs.** (**A**) RLU from LP02 Δ*flaA*Δ*uhpC* lux *L. pneumophila* (left) and Δ*flaA* lux *L. pneumophila* (right) from infected WT C57BL/6 BMMs stimulated with 6.0 ng/mL IFNγ ± 60.0 μM 3-bromopyruvate (3BP). (**C**) RLU from LP02 Δ*flaA*Δ*uhpC* lux *L. pneumophila* (left) and LP02 Δ*flaA* lux *L. pneumophila* (right) from infected WT C57BL/6 BMMs stimulated with 6.0 ng/mL IFNγ and 2.5 mM sodium oxamate (NaO). Data reflect results of individual experiments that represent at least three independent experiments. Error bars in all graphs represent mean ± standard deviation of at least two technical replicates. Concentrations of 3BP and NaO displayed represent the highest single point in a

820 titration at which we observed a minimum effect on *L. pneumophila* replication in the
821 absence of IFNγ.
822
823 **Supplementary Figure 2. 2DG triggers a transcriptional profile indicating**
824 **endoplasmic reticulum stress in IFNγ-stimulated BMMs.** (**A**) Heat map showing
825 fragments per kilobase million (FPKM) of differentially expressed transcripts measured
826 by RNAseq recovered from 1.0 x $10^6$ C57BL/6 BMMs/condition stimulated for 18 hours
827 with 50.0 ng/ml Pam3CSK4 + 2.0 ng/ml IFNγ ± 1.5 mM 2DG and 1.0 x $10^6$ C57BL/6
828 BMMs/condition infected at $T_0$ with LP02 Δ*flaA L. pneumophila* and stimulated 1 hour
829 post-infection with 2.0 ng/ml IFNγ ± 1.5 mM 2DG for a total of 18 hours prior to harvest.
830 Transcript IDs, FPKM, and $\log_2$ fold-change are shown in Supplementary Table 1. Only
831 transcripts shown to differ significantly between both Pam3CSK4/IFNγ and *L.p.*/IFNγ ±
832 2DG conditions, as calculated using TopHat/Cufflinks (57) are displayed. (**B**) $\text{Log}_{10}$ P-
833 value of gene ontology (GO) and comprehensive resource of mammalian protein
834 complexes (CORUM) gene sets in which transcripts significantly upregulated in + 2DG
835 conditions are enriched as determined using Metascape (59).
836
837 **Supplementary Figure 3. Validation of UPR gene expression by UPR stimuli and**
838 **inhibition of ATF4-dependent gene expression by ISRIB.** (**A**) Histograms displaying
839 transcripts per million (TPM) of *Hspa5* (heat shock protein 5, aka BIP), *Trib3* (tribbles
840 pseudokinase 3), *Dnajb3* (DnaJ heat shock protein family (Hsp40) member B3), *Pdia4*
841 (protein disulfide isomerase associated 4), *Manf* (mesencephalic astrocyte-derived
842 neurotrophic factor), and *Hyou1* (hypoxia up-regulated 1) measured by RNAseq

recovered from 1.0 x $10^6$ BMMs/condition stimulated for 18 hours with 100 ng/ml Pam3CSK4 (Pam) alone or in combination with 6.0 ng/ml IFNγ, IFNγ + 2.0 mM 2DG, IFNγ + 2.0 μM geldanamycin (Geld), IFNγ + 1.0 μg/ml brefeldin A (BfA), IFNγ + 2.0 mM dithiothreitol (DTT), IFNγ + 10.0 μM tunicamycin (Tunic), or IFNγ + 25.0 nM thapsigargin (Thaps). These genes are a subset associated with gene ontology term GO:0034976, response to endoplasmic reticulum stress. (**B**) Histograms displaying TPM of *Ddit3* (DNA-damage inducible transcript 3, aka CHOP), *Atf3* (activating transcription factor 3), and *Asns* (asparagine synthetase) measured by RNAseq recovered from 1.0 x $10^6$ BMMs/condition stimulated for 18 hours with 100 ng/ml Pam3CSK4 (Pam) alone or in combination with 6.0 ng/ml IFNγ, IFNγ + 2.0 mM 2DG, or IFNγ + 2.0 mM 2DG + 0.1 μM ISRIB. These genes are associated with PERK/ATF4-dependent gene expression (49).

**Supplementary Figure 4. *Nos2* and *Acod1* transcription segregates with conditions permissive and restrictive for *L. pneumophila* replication in BMMs.** (**A** and **B**) Histograms displaying transcripts per million (TPM) of *Nos2*, *Acod1*, *Irgm1*, *Irgm3*, *Cybb*, and *Casp11* measured by RNAseq recovered from 1.0 x $10^6$ BMMs/condition stimulated for 18 hours with 100 ng/ml Pam3CSK4 (Pam) alone or in combination with 6.0 ng/ml IFNγ, IFNγ + 2.0 mM 2DG, IFNγ + 2.0 μM geldanamycin (Geld), IFNγ + 1.0 μg/ml brefeldin A (BfA), IFNγ + 2.0 mM dithiothreitol (DTT), IFNγ + 10.0 μM tunicamycin (Tunic), IFNγ + 25.0 nM thapsigargin (Thaps).

**Supplementary Figure 5. Validation of CRISPR-mediated targeting of *Acod1* in iCas9 BMMs.** Western blot demonstrating loss of IRG1 protein expression in

iCas9::*Acod1* BMMs when stimulated for 24 hours with either 100 ng/ml *E. coli* lipopolysaccharide (LPS) or 100 ng/ml Pam3CSK4 + 10.0 ng/ml IFNγ. IRG1 migrates at ~53 kDa; the IRG1 antibody also stains a non-specific band at a slightly higher molecular weight. A separate antibody was used to stain for mouse β actin, which migrates at ~42 kDa.

Figure 1.

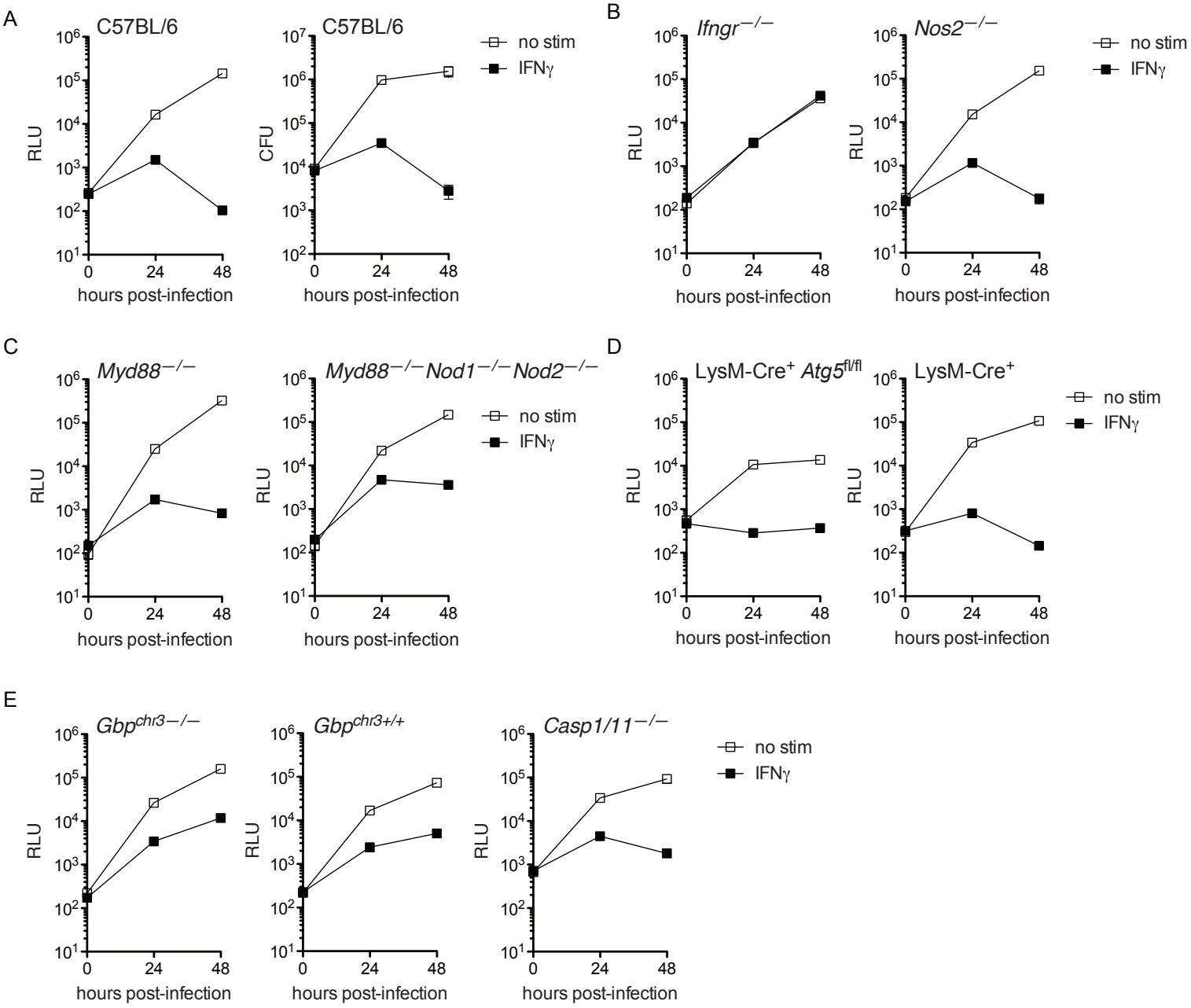

Figure 2.

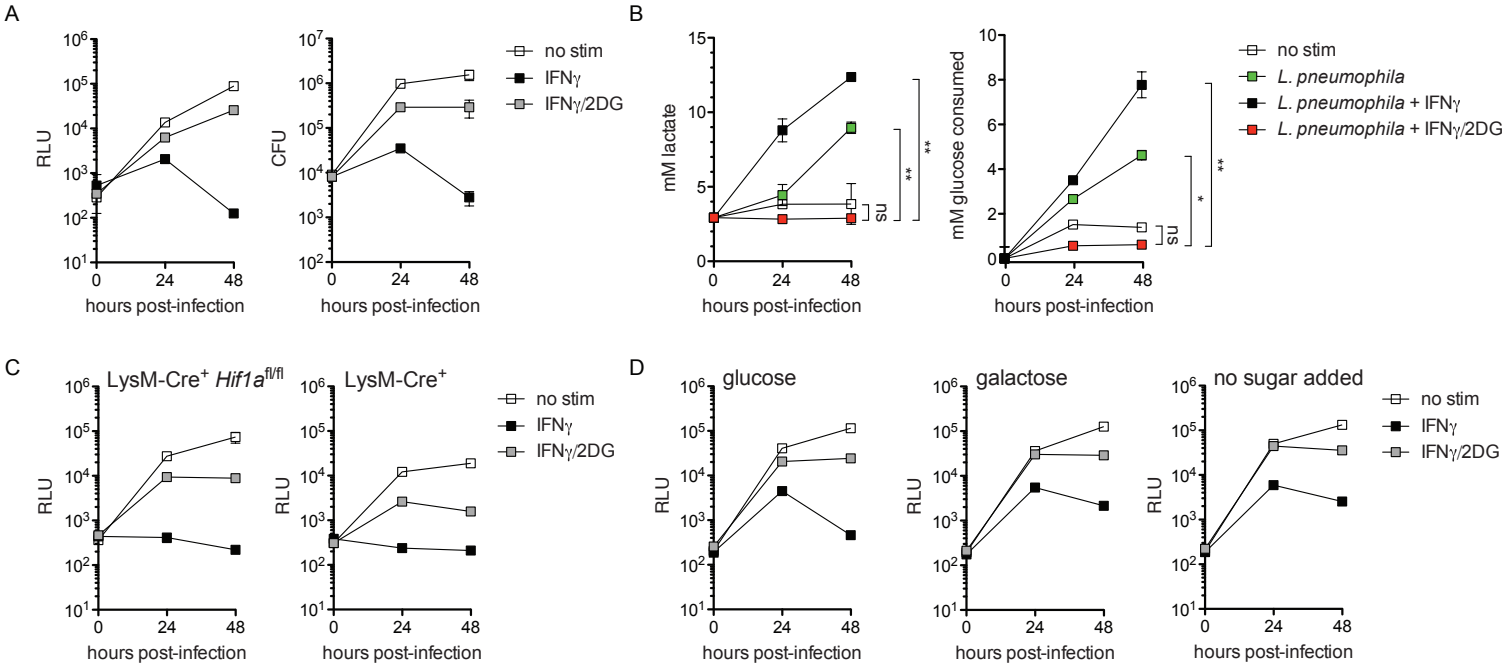

Figure 3.

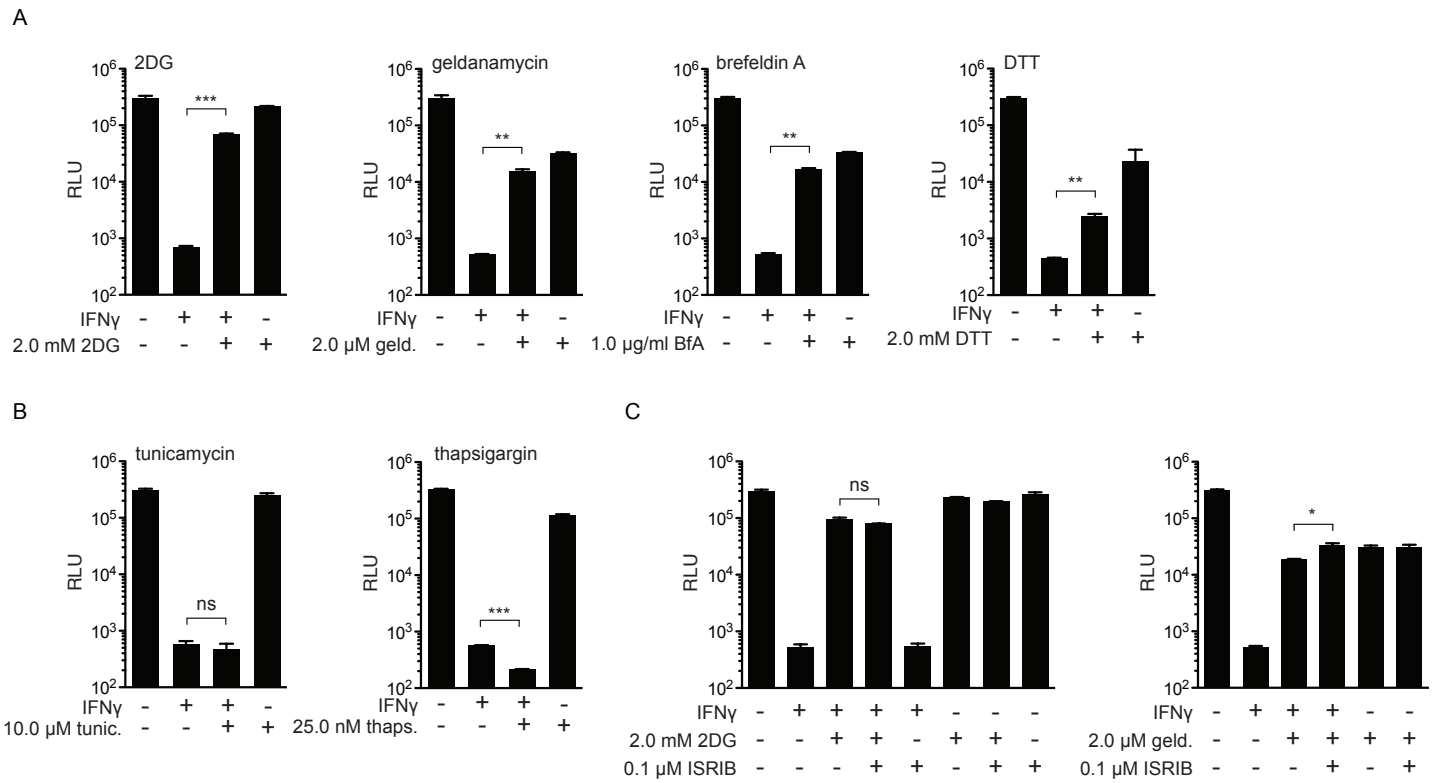

Figure 4.

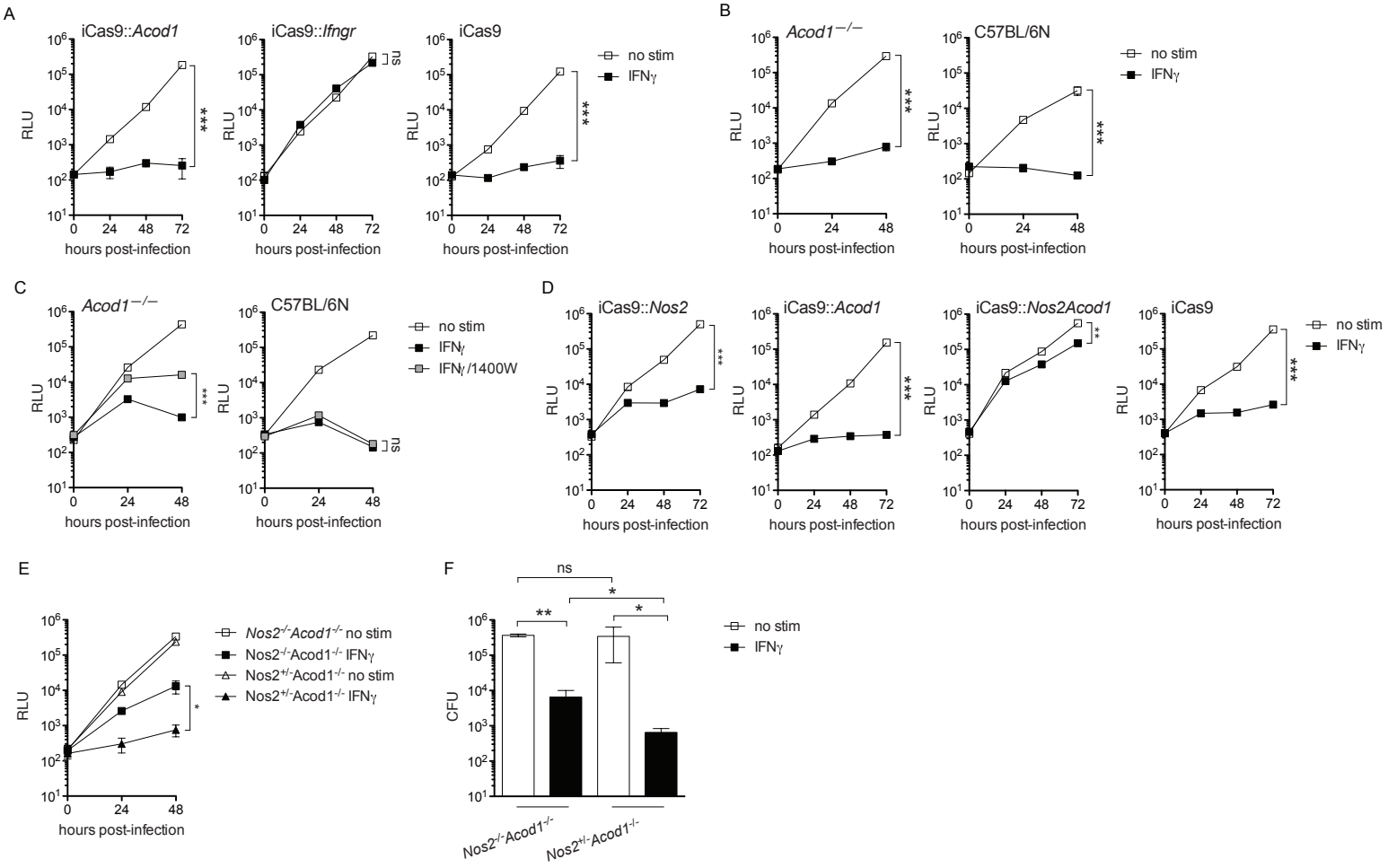

Figure 5.

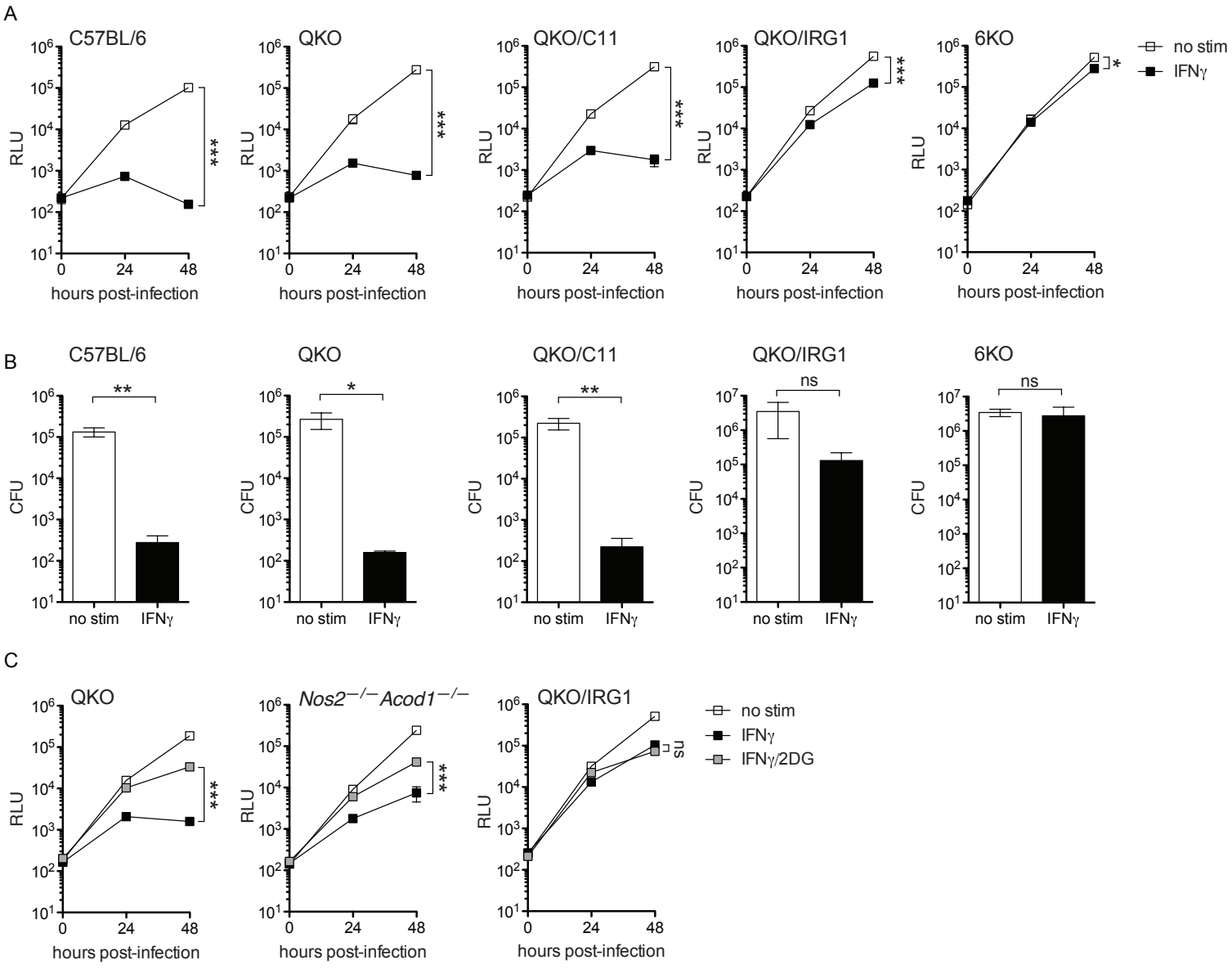

Table 1. Guide RNAs used in this study

CRISPR in iCas9 BMMs (requires gRNA sequence prepended with "G")

| **Guide RNA (gRNA) target:** | **gRNA sequence:** | **PAM:** | **Contributing to gentoype(s):** |
|---|---|---|---|
| *Ifngr* | GGTATTCCCAGCATACGACA | GGG | iCas9::*Ifngr* |
| *Acod1* exon 2 | GGACAGATGGTATCATTCGG | AGG | iCas9::*Acod1* ; iCas9::*Nos2Acod1* |
| *Acod1* exon 3 | GAAAAGCAGCATATGTCGGT | GGG | iCas9::*Acod1* ; iCas9::*Nos2Acod1* |
| *Nos2* exon 2 | GTCTTTCAGGTCACTTTGGT | AGG | iCas9::Nos2; iCas9::*Nos2Acod1* |
| *Nos2* intron 2-3 | GTCAGTAGTGACGTCCTGAT | TGG | iCas9::Nos2; iCas9::*Nos2Acod1* |

CRISPR in QKO mouse embryos

| **Guide RNA (gRNA) target:** | **gRNA sequence:** | **PAM:** | **Contributing to gentoype(s):** |
|---|---|---|---|
| *Acod1* exon 2 | TGACAGATGGTATCATTCGG | AGG | QKO/IRG1; 6KO |
| *Acod1* exon 3 | CAAAAGCAGCATATGTCGGT | GGG | QKO/IRG1; 6KO |
| Caspase11 exon 5 | GTATCATACTGTAGCACATC | TGG | QKO/C11; 6KO |
| Caspase11 intron 4-5 | ATGTTGATTTTACCGAAATG | AGG | QKO/C11; 6KO |

Supplementary Figure 1.

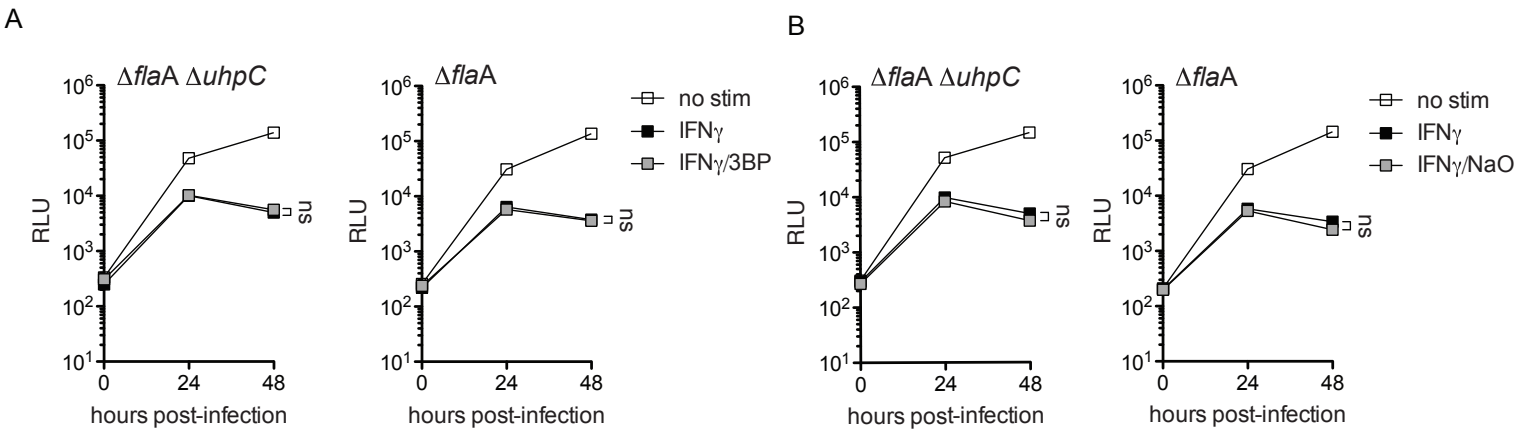

# Supplementary Fig. 2

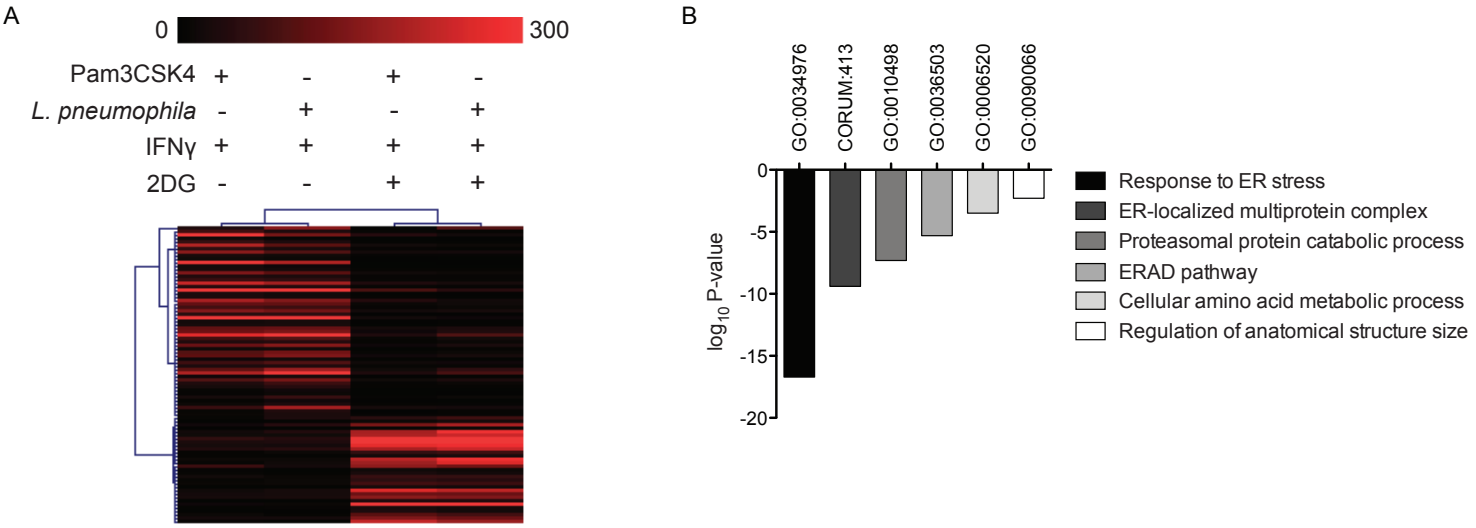

# Supplementary Fig. 3

A

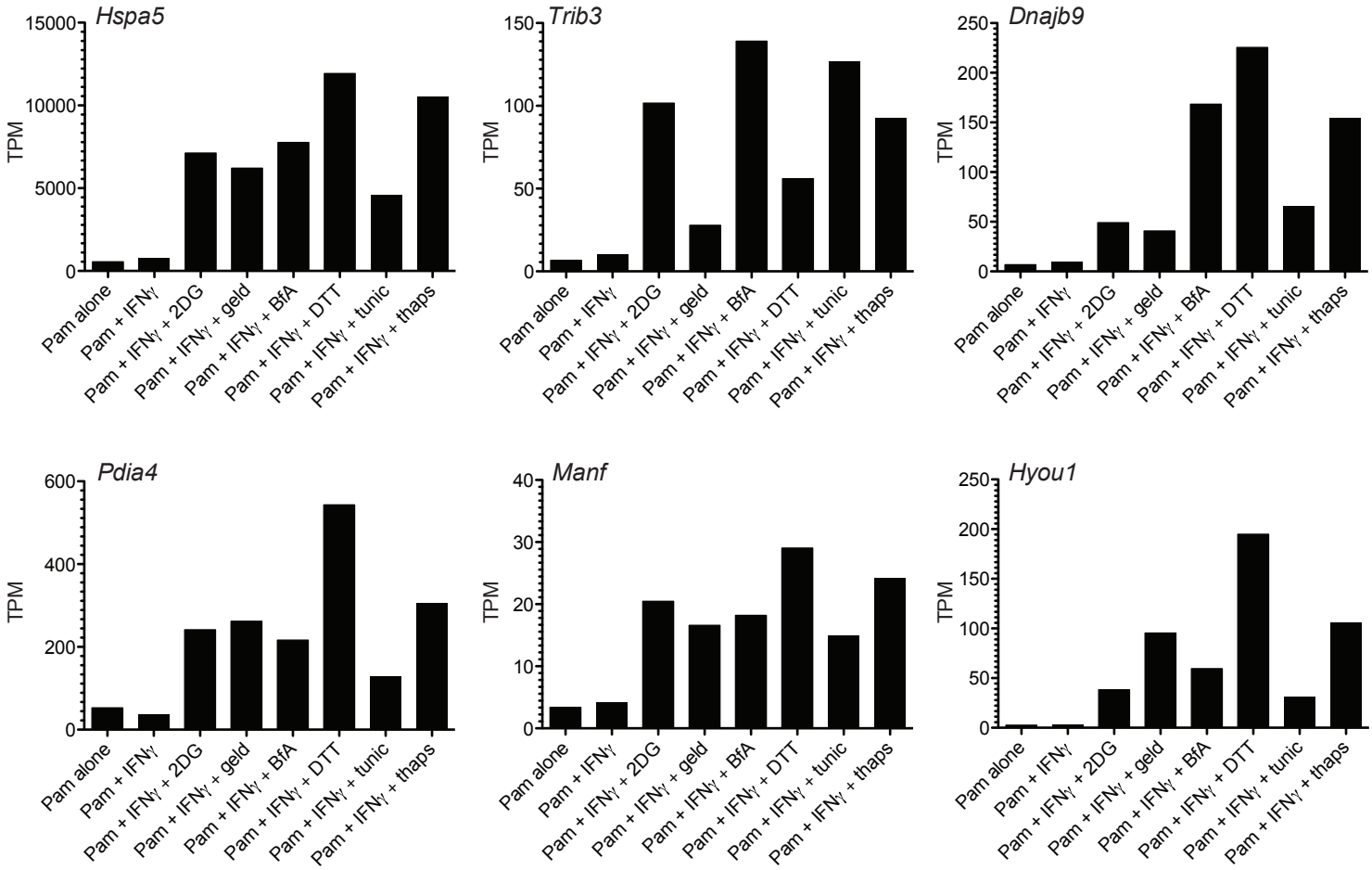


B

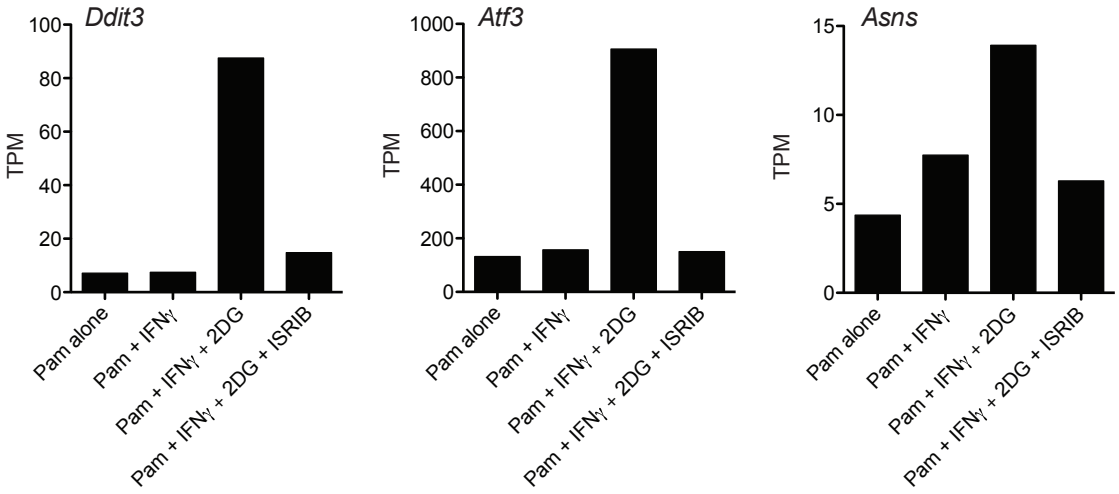

# Supplementary Fig. 4

A

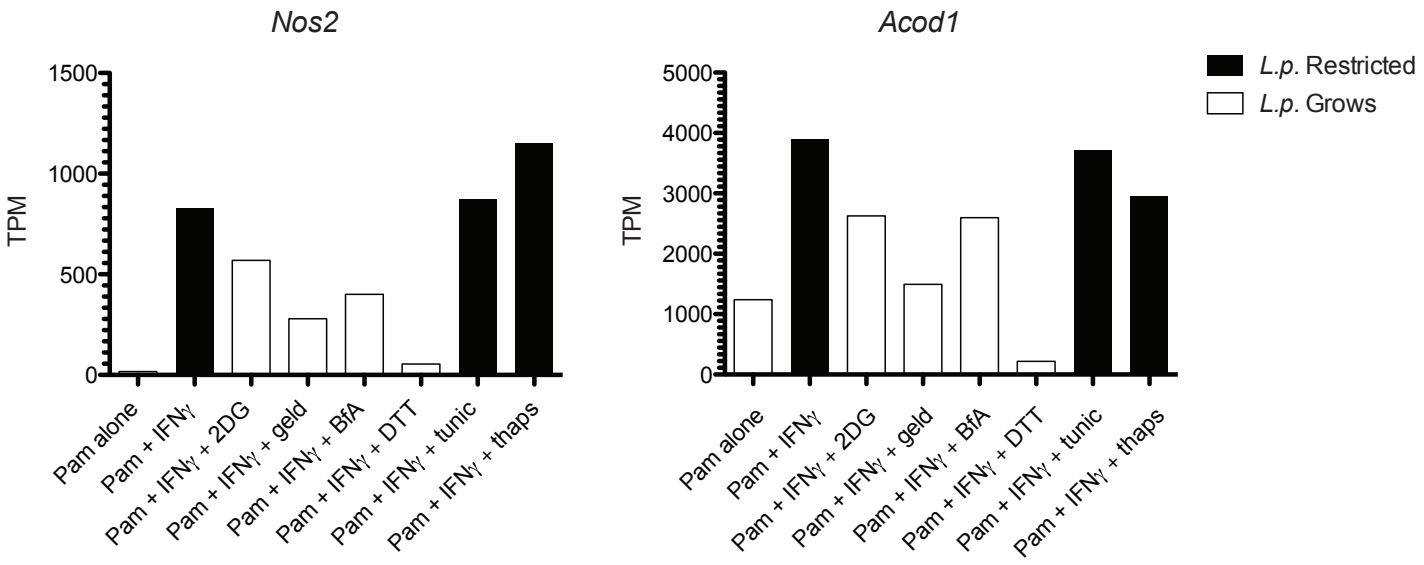


B

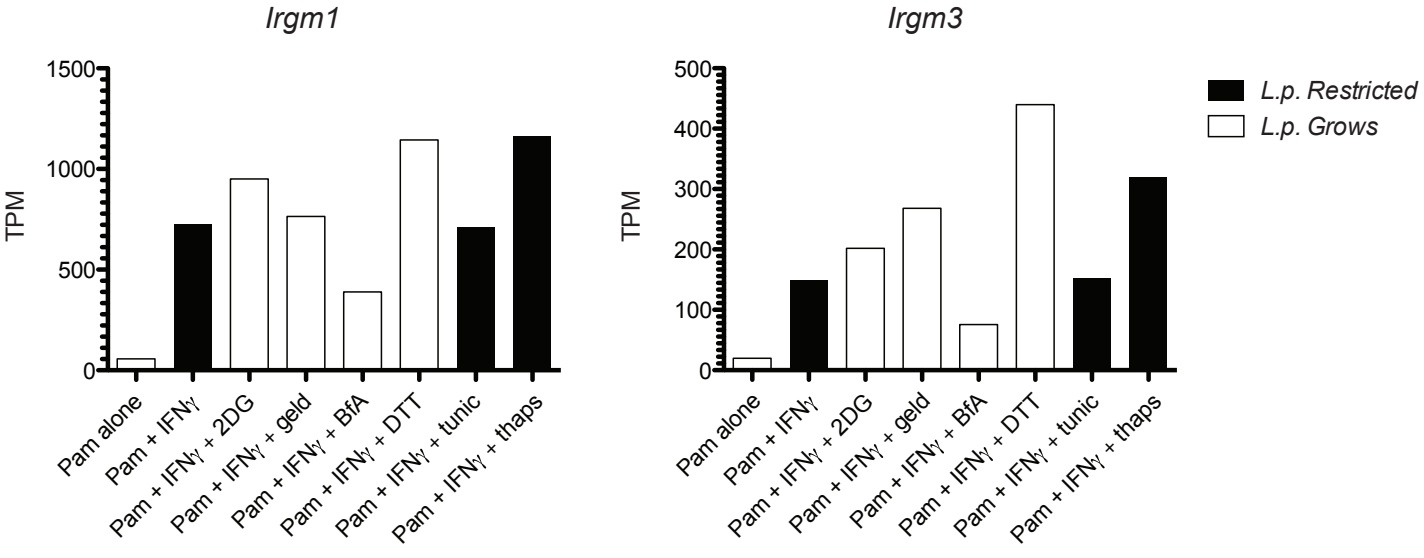


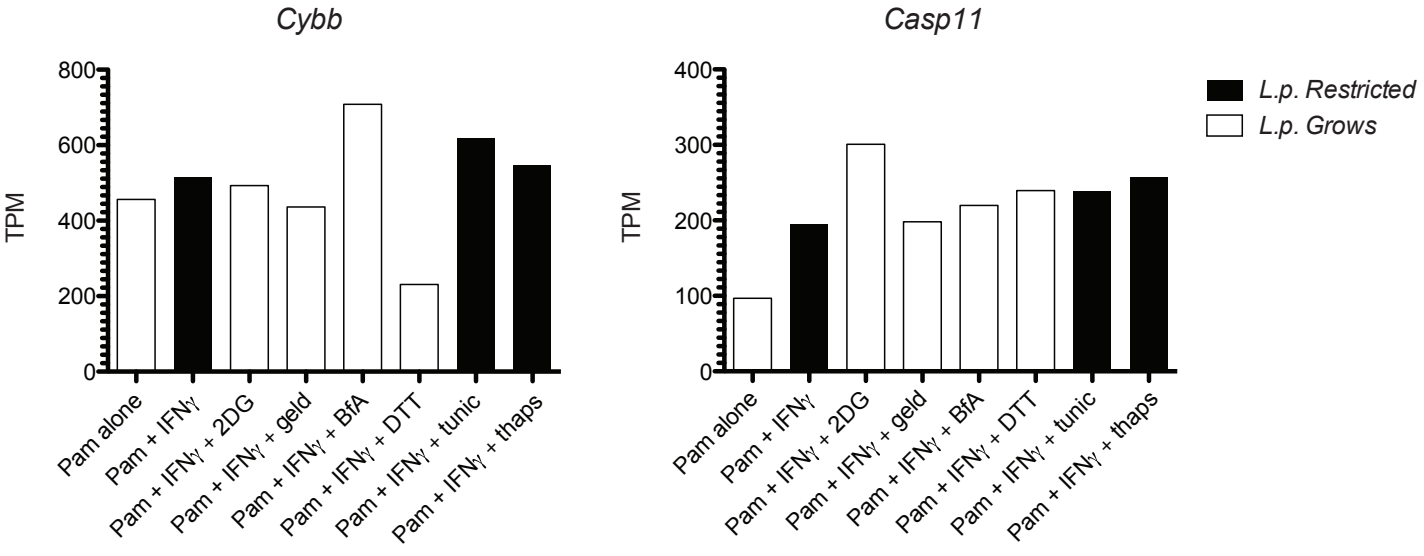

Supplementary Figure 5.

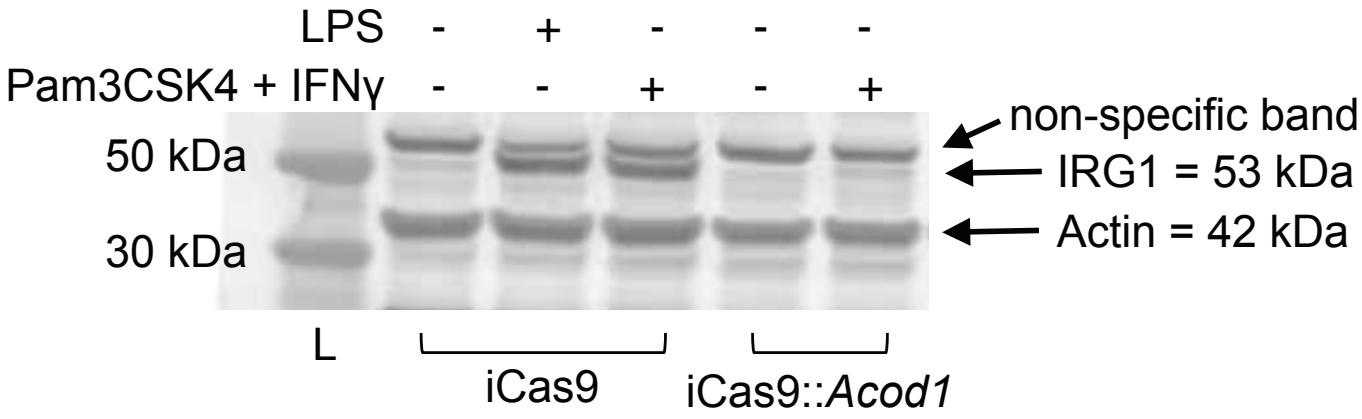

Supplementary Table 1. Transcripts that vary significantly in BMMs treated with Pam3CSK4 + IFNγ vs. Pam3CSK4 + IFNγ + 2DG

| Location | PAM+IFNγ FPKM | *L.p.*+IFNγ FPKM | PAM+IFNγ+2DG FPKM | *L.p.*+IFNγ+2DG FPKM | log2 fold change PAM | log2 fold change *L.p.* | Gene |
|---|---|---|---|---|---|---|---|
| chr3:121723536-121735052 | 8.64 | 40.80 | 0.00 | 5.34 | #DIV/0! | 2.93 | F3 |
| chr10:24914852-24927760 | 330.60 | 207.90 | 2.82 | 1.73 | 6.87 | 6.91 | Arg1 |
| chr10:99263230-99267489 | 51.60 | 57.56 | 1.67 | 2.19 | 4.95 | 4.72 | Dusp6 |
| chr11:9117979-9136170 | 378.41 | 400.15 | 22.16 | 16.15 | 4.09 | 4.63 | Upp1 |
| chr8:65618039-66473349 | 65.13 | 33.38 | 4.18 | 4.00 | 3.96 | 3.06 | March1 |
| chr12:119158487-119238276 | 19.50 | 12.96 | 1.64 | 2.44 | 3.57 | 2.41 | Itgb8 |
| chr13:60895350-60897447 | 98.59 | 132.14 | 9.22 | 13.67 | 3.42 | 3.27 | Ctla2b |
| chr2:128698860-128803160 | 22.88 | 25.86 | 2.16 | 3.90 | 3.40 | 2.73 | Mertk |
| chr13:117220572-117274415 | 81.92 | 73.16 | 7.79 | 12.61 | 3.39 | 2.54 | Emb |
| chr5:43868826-43912389 | 208.64 | 107.66 | 20.31 | 14.14 | 3.36 | 2.93 | Cd38 |
| chr14:60634728-60764556 | 26.37 | 27.59 | 2.65 | 5.08 | 3.32 | 2.44 | Spata13 |
| chr9:124102182-124109140 | 15.99 | 25.65 | 1.63 | 4.28 | 3.29 | 2.58 | Ccr2 |
| chr16:10782304-10785536 | 115.02 | 113.26 | 12.45 | 18.68 | 3.21 | 2.60 | Socs1 |
| chr7:43526933-43533175 | 30.95 | 22.50 | 3.38 | 1.66 | 3.20 | 3.76 | Cd33 |
| chr12:32173396-32208649 | 25.18 | 16.27 | 3.00 | 2.38 | 3.07 | 2.77 | Pik3cg |
| chr4:132732965-132757171 | 147.14 | 106.91 | 17.72 | 14.48 | 3.05 | 2.88 | Smpdl3b |
| chr5:123863569-123865516 | 79.28 | 95.76 | 9.69 | 20.41 | 3.03 | 2.23 | Niacr1 |
| chr10:56377299-56390419 | 76.79 | 35.79 | 9.43 | 5.28 | 3.03 | 2.76 | Gja1 |
| chr13:43785106-43803132 | 37.04 | 157.83 | 4.70 | 98.43 | 2.98 | 0.68 | Cd83 |
| chr6:29272487-29276390 | 127.10 | 143.20 | 16.23 | 38.78 | 2.97 | 1.88 | Hilpda |
| chr19:40659646-40742515 | 39.22 | 47.47 | 5.09 | 11.21 | 2.94 | 2.08 | Entpd1 |
| chr10:10335702-10472314 | 55.22 | 30.34 | 7.18 | 4.46 | 2.94 | 2.77 | Adgb |
| chr11:62248983-62266580 | 123.70 | 155.86 | 16.22 | 29.61 | 2.93 | 2.40 | Adora2b |
| chr5:43818892-43843468 | 71.44 | 57.94 | 9.40 | 9.24 | 2.93 | 2.65 | Bst1 |
| chr9:7272513-7283333 | 352.87 | 137.78 | 47.51 | 22.29 | 2.89 | 2.63 | Mmp13 |
| chr11:117965741-117969830 | 262.49 | 306.84 | 35.50 | 94.93 | 2.89 | 1.69 | Socs3 |
| chr6:123227866-123247024 | 151.03 | 133.87 | 21.24 | 26.78 | 2.83 | 2.32 | Clec4n |
| chr7:3485746-3502752 | 159.87 | 96.29 | 23.43 | 23.92 | 2.77 | 2.01 | Tarm1 |
| chr13:97241104-97253040 | 17.85 | 23.35 | 2.74 | 5.14 | 2.71 | 2.18 | Enc1 |
| chr11:83116844-83122659 | 109.82 | 148.71 | 17.36 | 26.50 | 2.66 | 2.49 | Slfn1 |
| chr17:17887823-17893952 | 569.21 | 405.70 | 90.54 | 49.52 | 2.65 | 3.03 | Fpr2 |
| chr17:17875768-17883951 | 233.86 | 190.30 | 38.79 | 25.60 | 2.59 | 2.89 | Fpr1 |
| chr12:31958478-32061279 | 31.62 | 24.11 | 5.41 | 3.49 | 2.55 | 2.79 | Prkar2b |
| chr12:85473900-85477478 | 109.40 | 181.78 | 19.23 | 57.55 | 2.51 | 1.66 | Fos |
| chr2:117279992-117342877 | 28.14 | 21.39 | 5.01 | 5.37 | 2.49 | 1.99 | Rasgrp1 |
| chr18:60393061-60443899 | 38.13 | 72.99 | 6.80 | 12.16 | 2.49 | 2.59 | EMBL-EBI AK149718.1 |
| chr15:74979722-75048837 | 203.51 | 318.72 | 37.53 | 87.21 | 2.44 | 1.87 | Ly6a |
| chr9:118606708-118901003 | 18.55 | 6.20 | 3.48 | 2.30 | 2.42 | 1.43 | Itga9 |
| chr2:164948238-164955846 | 40.93 | 31.23 | 7.80 | 7.27 | 2.39 | 2.10 | Mmp9 |
| chr16:75858793-75909273 | 96.32 | 139.27 | 18.98 | 32.44 | 2.34 | 2.10 | Samsn1 |
| chr7:38183216-38197565 | 26.84 | 48.18 | 5.34 | 5.68 | 2.33 | 3.09 | RIKEN cDNA 1600014C10 |
| chr4:132781761-132796364 | 112.02 | 119.12 | 22.44 | 31.54 | 2.32 | 1.92 | Themis2 |
| chr19:21778341-21858450 | 48.39 | 42.18 | 9.98 | 6.90 | 2.28 | 2.61 | Cemip2 |
| chr9:41012959-41157668 | 29.20 | 18.98 | 6.47 | 6.32 | 2.17 | 1.59 | Ubash3b |
| chr5:137787801-137858049 | 197.74 | 153.77 | 44.00 | 22.16 | 2.17 | 2.79 | Zcwpw1 |
| chr12:80107759-80113013 | 16.27 | 22.12 | 3.87 | 2.84 | 2.07 | 2.96 | Zfp36l1 |
| chr8:92855349-92919279 | 75.81 | 97.27 | 18.55 | 17.46 | 2.03 | 2.48 | Lpcat2 |
| chr11:48985328-48992246 | 26.32 | 69.92 | 6.72 | 13.40 | 1.97 | 2.38 | Tgtp1 |
| chr11:44454570-44470548 | 34.39 | 40.38 | 9.35 | 8.33 | 1.88 | 2.28 | Ublcp1 |
| chr7:114415253-114538029 | 9.19 | 16.69 | 2.59 | 2.62 | 1.83 | 2.67 | Pde3b |
| chr3:27317076-27339665 | 5.40 | 16.81 | 1.74 | 2.59 | 1.64 | 2.70 | Tnfsf10 |
| chr17:44096293-44105808 | 8.18 | 14.92 | 2.71 | 2.14 | 1.60 | 2.80 | Enpp4 |
| chr8:45395664-45410539 | 15.12 | 33.76 | 5.17 | 6.57 | 1.55 | 2.36 | Tlr3 |
| chr11:83175185-83190251 | 71.33 | 191.83 | 26.41 | 24.21 | 1.43 | 2.99 | Slfn4 |
| chr19:21391306-21472661 | 11.06 | 32.62 | 6.57 | 6.32 | 0.75 | 2.37 | Gda |
| chr6:7675170-7693182 | 73.21 | 24.00 | 165.25 | 132.37 | -1.17 | -2.46 | Asns |
| chr4:59805649-59904832 | 5.90 | 2.86 | 17.84 | 14.42 | -1.60 | -2.33 | Snx30 |
| chrX:36328408-36366856 | 9.53 | 4.48 | 30.18 | 22.38 | -1.66 | -2.32 | Lonrf3 |
| chr3:108424774-108445259 | 20.26 | 12.28 | 70.09 | 65.73 | -1.79 | -2.42 | Sars |
| chr3:100468062-100489192 | 3.45 | 3.65 | 14.71 | 26.76 | -2.09 | -2.87 | Fam46c |
| chr10:127514938-127522444 | 5.23 | 4.16 | 22.87 | 29.79 | -2.13 | -2.84 | Shmt2 |
| chr16:22857844-22879634 | 39.83 | 50.36 | 195.50 | 234.30 | -2.30 | -2.22 | Dnajb11 |
| chr12:116405401-116463531 | 1.97 | 2.87 | 9.82 | 14.79 | -2.32 | -2.36 | Ncapg2 |
| chr7:132557474-132576398 | 24.59 | 26.95 | 127.96 | 123.99 | -2.38 | -2.20 | Oat |
| chr11:114922780-114934386 | 9.25 | 13.23 | 53.38 | 47.90 | -2.53 | -1.86 | Cd300lb |
| chr2:121413901-121438686 | 24.63 | 23.63 | 149.03 | 124.87 | -2.60 | -2.40 | Pdia3 |
| chr12:91805907-91849157 | 26.09 | 27.07 | 159.39 | 150.35 | -2.61 | -2.47 | Sel1l |
| chr7:45522738-45526268 | 8.36 | 35.02 | 51.65 | 77.48 | -2.63 | -1.15 | Ppp1r15a |
| chr14:118937931-118981702 | 12.60 | 14.45 | 82.25 | 73.67 | -2.71 | -2.35 | Dnajc3 |
| chr13:95627176-95891922 | 3.81 | 7.23 | 27.27 | 22.09 | -2.84 | -1.61 | Iqgap2 |
| chr2:152337424-152344060 | 13.31 | 5.55 | 106.51 | 83.01 | -3.00 | -3.90 | Trib3 |
| chr18:65800577-65817657 | 16.65 | 48.02 | 140.92 | 196.46 | -3.08 | -2.03 | Sec11c |
| chr13:110395043-110400843 | 21.74 | 43.21 | 195.08 | 288.27 | -3.17 | -2.74 | Plk2 |
| chr12:17266594-17324730 | 61.82 | 47.19 | 606.19 | 664.54 | -3.29 | -3.82 | Pdia6 |
| chr14:103814624-103844524 | 2.83 | 2.98 | 27.82 | 24.59 | -3.30 | -3.04 | Ednrb |
| chr9:106887414-106891938 | 19.43 | 19.31 | 201.31 | 236.22 | -3.37 | -3.61 | Manf |
| chr6:47796140-47813512 | 31.57 | 35.74 | 330.67 | 344.11 | -3.39 | -3.27 | Pdia4 |
| chr9:44379489-44392576 | 24.95 | 23.65 | 269.93 | 281.33 | -3.44 | -3.57 | Hyou1 |
| chr16:92391952-92466146 | 5.64 | 13.03 | 63.96 | 77.68 | -3.50 | -2.58 | Rcan1 |
| chr2:84936608-84958509 | 3.33 | 2.78 | 41.74 | 39.64 | -3.65 | -3.84 | Slc43a3 |
| chr12:83987860-83993875 | 2.60 | 1.65 | 33.74 | 23.37 | -3.70 | -3.83 | Acot2 |
| chr12:44205896-44210068 | 17.95 | 25.83 | 259.96 | 223.40 | -3.86 | -3.11 | Dnajb9 |
| chr10:127290792-127311786 | 14.13 | 14.59 | 217.63 | 284.18 | -3.94 | -4.28 | Ddit3 |
| chr15:88819645-88826718 | 10.05 | 18.32 | 184.55 | 257.10 | -4.20 | -3.81 | Creld2 |
| chr16:17130137-17132383 | 15.35 | 11.96 | 331.95 | 311.42 | -4.43 | -4.70 | Sdf2l1 |
| chr8:94386499-94395358 | 6.33 | 3.36 | 225.67 | 175.88 | -5.16 | -5.71 | Herpud1 |